

Quantum Transport in Interacting Spin Chains: Exact Derivation of the GUE Tracy-Widom Distribution

Kazuya Fujimoto¹ and Tomohiro Sasamoto¹

¹*Department of Physics, Institute of Science Tokyo,
2-12-1 Ookayama, Meguro-ku, Tokyo 152-8551, Japan*

(Dated: December 31, 2024)

We theoretically study quantum spin transport in a one-dimensional folded XXZ model with an alternating domain-wall initial state via the Bethe ansatz technique, exactly demonstrating that a probability distribution of finding a left-most up-spin with an appropriate scaling variable converges to the Tracy-Widom distribution for the Gaussian unitary ensemble (GUE), which is a universal distribution for the largest eigenvalue of GUE under a soft-edge scaling limit. Our finding presented here offers a first exact derivation of the GUE Tracy-Widom distribution in the dynamics of the interacting quantum model not being mapped to a noninteracting fermion Hamiltonian via the Jordan-Wigner transformation. On the basis of the exact solution of the folded XXZ model and our numerical analysis of the XXZ model, we discuss a universal behavior for the probability of finding the left-most up-spin in the XXZ model.

Introduction.— Transport of a physical quantity is ubiquitous both for classical and quantum systems, having played pivotal roles in deepening our understanding of many-body dynamics over decades [1–4]. One of the notable achievements in classical transport is the establishment of the celebrated Kardar-Parisi-Zhang (KPZ) universality [5–9], which was originally developed in classical statistical mechanics for growing surface physics [10] and transport of stochastic processes [11, 12]. When a stochastic system belongs to the KPZ universality, the integrated particle current are universally characterized by the Tracy-Widom distribution of random matrix theory, which is a universal distribution for the largest eigenvalue of random matrices [13–16]. Recently, such universal transport featuring random matrix theory and the KPZ universality is intensively explored in quantum regimes from theoretical [17–28] and experimental [29–31] perspectives, having been recognized as an important research subject in quantum many-body systems.

One of intriguing exact results for quantum transport featuring random matrix theory is emergence of the Tracy-Widom distribution in a one-dimensional XX model being equivalent to noninteracting fermions [32, 33]. The previous works of Refs. [32, 33] consider quantum spin transport starting from a domain-wall state, uncovering that a probability $P(x, t)$ for the farthest up-spin at site x and time t obeys the GUE Tracy-Widom distribution [13, 15, 16], which is the universal distribution for the largest eigenvalue in the Gaussian unitary ensemble (GUE) of random matrix theory. After this finding, several numerical works [34, 35] studied impact of interactions on the quantum dynamics using a one-dimensional XXZ model, which is mapped into an interacting fermions, and then reported a signature for absence of the GUE Tracy-Widom behavior. On the other hand, Bulchandani and Karrasch reported tendencies for presence of the GUE Tracy-Widom behavior [36]. On the mathematical side, Saenz, Tracy, and Widom conducted pioneering and laborious analysis for

the probability $P(x, t)$ in the XXZ model via the Bethe ansatz [37, 38], proposing an important conjecture concerning a scaling limit for $P(x, t)$ [33]. However, exact derivation of the GUE Tracy-Widom distribution in the XXZ model has yet to be completed. Therefore, it has been elusive whether the GUE Tracy-Widom behavior can survive in interacting quantum many-body systems.

In this Letter, we present a first example for exactly deriving the GUE Tracy-Widom distribution in an interacting quantum spin model on a one-dimensional lattice, namely a folded XXZ model [39–44], which cannot be mapped into a noninteracting fermion Hamiltonian via the Jordan-Wigner transformation [45, 46]. This theoretical model is originally derived as an effective Hamil-

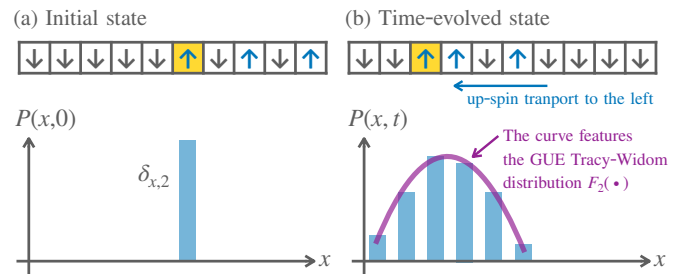


FIG. 1. Schematic illustration for the main result of this Letter. The prime quantity of our interest is a probability $P(x, t)$ of finding a left-most up spin at site x and time t , which is emphasized by the yellow-color cell. (a) Initial spin configuration and probability $P(x, 0)$. The initial state is an alternating domain-wall state, where the up spins occupy every other sites in half of the system ($x \geq 2$). By definition, we have $P(x, 0) = \delta_{x,2}$ (see Eqs. (2) and (3)). (b) Time-evolved spin configuration and probability $P(x, t)$ at time t . After the unitary time-evolution with the folded XXZ model, the up-spins are transported to the left region ($x < 2$). In this Letter, we demonstrate that the rescaled probability $P(x, t)$ converges to a probability density function for the GUE Tracy-Widom distribution function $F_2(\bullet)$ [13, 15, 16] in the long-time limit.

tonian for the XXZ model with the large anisotropic interaction. Using the folded XXZ model, we theoretically study quantum spin transport starting from an alternating domain-wall state where the up-spin occupies half of the system every other site as depicted in Fig. 1(a). We employ exact analysis based on the Bethe ansatz [37, 38], analytically showing that the rescaled probability $P(x, t)$ of finding the left-most up-spin at site x and time t converges to a probability density function for the GUE Tracy-Widom distribution function $F_2(\bullet)$ in the long-time limit. Figure 1(b) schematically illustrates this result. Beyond the folded XXZ model, we numerically investigate the XXZ model via the time-evolving decimation method (TEBD) [47–50], discussing signatures for a universal behavior of $P(x, t)$ in the XXZ model.

Setup.— We consider an infinite lattice, sites of which are labeled by \mathbb{Z} , and denote spin-1/2 operators at site $w \in \mathbb{Z}$ by \hat{X}_w, \hat{Y}_w and \hat{Z}_w in the x, y , and z directions, respectively. These operators satisfy SU(2) commutation relations, e.g., $[\hat{X}_x, \hat{Y}_y] = i\hat{Z}_x \delta_{x,y}$, where we set the Dirac constant \hbar to be unity. Under this setup, we consider the Hamiltonian of the folded XXZ model [39–44], which is defined by

$$\hat{H}_{\text{fXXZ}} := \sum_{x \in \mathbb{Z}} (\hat{X}_x \hat{X}_{x+1} + \hat{Y}_x \hat{Y}_{x+1}) \frac{1 + 4\hat{Z}_{x-1} \hat{Z}_{x+2}}{2}. \quad (1)$$

This is the effective Hamiltonian for the XXZ model with the large anisotropic interaction $\Delta \gg 1$. Here, the Hamiltonian for the XXZ model is given by $\hat{H}_{\text{XXZ}} := \sum_{x \in \mathbb{Z}} (\hat{X}_x \hat{X}_{x+1} + \hat{Y}_x \hat{Y}_{x+1} + \Delta \hat{Z}_x \hat{Z}_{x+1})$ with the parameter Δ being responsible for the spin interaction in the z -direction. We denote the quantum state by $|\phi(t)\rangle$ and assume that it obeys the Schrödinger equation, $id|\phi(t)\rangle/dt = \hat{H}_{\text{fXXZ}}|\phi(t)\rangle$. The initial state considered in this work is the alternating domain-wall state defined by

$$|\phi(0)\rangle = \prod_{x=1}^N \hat{R}_{2x} |0\rangle \quad (2)$$

with the vacuum $|0\rangle$ representing all the down-spin state, the raising operator $\hat{R}_x := \hat{X}_x + i\hat{Y}_x$, and the total number N of the up-spins. Figure 1(a) displays the schematic illustration for this initial state. Since \hat{H}_{fXXZ} conserves

the total up-spin, we can expand the quantum state as $|\phi(t)\rangle = \sum_{\mathbf{x}: x_j < x_{j+1}} \Phi(x_1, \dots, x_N, t) |x_1, \dots, x_N\rangle$, where x_j ($j \in \{1, \dots, N\}$) is a lattice site occupied by an up-spin and $\Phi(x_1, \dots, x_N, t)$ is the many-body wavefunction in the basis $|x_1, \dots, x_N\rangle := \prod_{j=1}^N \hat{R}_{x_j} |0\rangle$.

The quantity of our interest is the probability $P(x, t)$ of finding the left-most up-spin at site x and time t , which is defined by

$$P(x, t) := \sum_{y_2=1}^{\infty} \cdots \sum_{y_N=1}^{\infty} \left| \Phi \left(x, x + y_2, \dots, x + \sum_{j=2}^N y_j, t \right) \right|^2. \quad (3)$$

The corresponding complementary cumulative distribution function $F(x, t)$ is defined by

$$F(x, t) := \sum_{y=x}^{\infty} P(y, t). \quad (4)$$

In what follows, we shall prove that $F(x, t)$ converges to the GUE Tracy-Widom distribution function in the long-time limit.

Determinantal formula of $F(x, t)$ via the Bethe ansatz.— We shall derive a determinantal expression for $F(x, t)$ using the Bethe ansatz [37, 38] because the folded XXZ model is Bethe solvable [40–42].

We first derive an integral formula for $\Phi(x_1, \dots, x_N, t)$ by using the Bethe-ansatz method developed by Schütz [51], Tracy and Widom [52]. As described in Sec. I of the Supplemental Material (SM) [53], we obtain

$$\Phi(x_1, \dots, x_N, t) = \int_{C_r} d\boldsymbol{\xi} \sum_{\sigma \in \mathbb{S}_N} A_{\sigma}(\boldsymbol{\xi}) \prod_{j=1}^N \xi_{\sigma_j}^{x_j - 2\sigma_j - 1} e^{-iE_{\xi_j} t} \quad (5)$$

with the set \mathbb{S}_N for N th permutations and the multiple complex integral $\int_{C_r} d\boldsymbol{\xi} := (2\pi i)^{-N} \int_{C_r} d\xi_1 \cdots \int_{C_r} d\xi_N$, and $E_{\xi} := (\xi + \xi^{-1})/2$. The contour C_r is a circle encircling the origin in the complex plane and its radius r is strictly smaller than unity. The coefficient $A_{\sigma}(\boldsymbol{\xi})$ is defined by $A_{\sigma}(\boldsymbol{\xi}) := \prod_{(j,k) \in \mathcal{A}_{\sigma}} S(\xi_j, \xi_k)$, where \mathcal{A}_{σ} is a set for (j, k) such that (j, k) are an inversion in a given element σ of \mathbb{S}_N . The scattering amplitude is given by $S(\xi_j, \xi_k) := -\xi_j/\xi_k$ [40–42].

We next calculate $F(x, t)$ by using Eq. (5). By definition, we get the expression of $P(x, t)$ as

$$P(x, t) = \sum_{\sigma \in \mathbb{S}_N} \sum_{\mu \in \mathbb{S}_N} \int_{C_r} d\boldsymbol{\xi} \int_{C_r} d\boldsymbol{\eta} \frac{A_{\sigma}(\boldsymbol{\xi}) A_{\mu}(\boldsymbol{\eta}) \prod_{j=1}^{N-1} (\xi_{\sigma_{j+1}} \eta_{\mu_{j+1}})^j}{\prod_{j=1}^{N-1} (1 - \prod_{k=j+1}^N \xi_{\sigma_k} \eta_{\mu_k})} \prod_{j=1}^N [(\xi_j \eta_j)^{x-2j-1} e^{-it(E_{\xi_j} - E_{\eta_j})}]. \quad (6)$$

To derive this expression, we use the fact that $\Phi(x_1, \dots, x_N, t)$ vanishes if there exists a site label j such that $x_j = x_{j+1} + 1$ is satisfied (see the derivation of this

property in Sec. II of SM [53]). To compute the summations over σ and μ in Eq. (6), we note the following identity [33, 54, 55] being related to the Izergin-Korepin

determinant of the six-vertex model [56–59],

$$\begin{aligned} & \sum_{\sigma \in \mathbb{S}_N} \sum_{\mu \in \mathbb{S}_N} \frac{B_\sigma(\boldsymbol{\xi}) B_\mu(\boldsymbol{\eta}) \prod_{j=1}^{N-1} (\xi_{\sigma_{j+1}} \eta_{\mu_{j+1}})^j}{\prod_{j=1}^{N-1} (1 - \prod_{k=j+1}^N \xi_{\sigma_k} \eta_{\mu_k})} \\ &= \frac{(1 - \prod_{j=1}^N \xi_j \eta_j) \prod_{j,k=1}^N (\xi_j + \eta_k - 2\Delta \xi_j \eta_k)}{\prod_{j < k} (1 + \xi_j \xi_k - 2\Delta \xi_j) (1 + \eta_j \eta_k - 2\Delta \eta_j)} D_N(\boldsymbol{\xi}, \boldsymbol{\eta}), \end{aligned} \quad (7)$$

where we define $D_N(\boldsymbol{\xi}, \boldsymbol{\eta}) := \det(d(\xi_j, \eta_k))_{j,k \in \{1, \dots, N\}}$ with $d(\xi_j, \eta_k) := (1 - \xi_j \eta_k)^{-1} (\xi_j + \eta_k - 2\Delta \xi_j \eta_k)^{-1}$. The function $B_\sigma(\boldsymbol{\xi})$ is defined by $B_\sigma(\boldsymbol{\xi}) := \prod_{(j,k) \in A_\sigma} S_{\text{XXZ}}(\xi_j, \xi_k)$ with the scattering amplitude $S_{\text{XXZ}}(\xi_j, \xi_k) := -(1 + \xi_j \xi_k - \Delta \xi_j) / (1 + \xi_j \xi_k - \Delta \xi_k)$ for the XXZ model [37, 38]. We can easily show $\lim_{\Delta \rightarrow \infty} B_\sigma(\boldsymbol{\xi}) = A_\sigma(\boldsymbol{\xi})$. Thus, taking the limit $\Delta \rightarrow \infty$ in Eq. (7), we derive

$$\begin{aligned} & \sum_{\sigma \in \mathbb{S}_N} \sum_{\mu \in \mathbb{S}_N} \frac{A_\sigma(\boldsymbol{\xi}) A_\mu(\boldsymbol{\eta}) \prod_{j=1}^{N-1} (\xi_{\sigma_{j+1}} \eta_{\mu_{j+1}})^j}{\prod_{j=1}^{N-1} (1 - \prod_{k=j+1}^N \xi_{\sigma_k} \eta_{\mu_k})} \\ &= \left(1 - \prod_{j=1}^N \xi_j \eta_j \right) \det \left(\frac{(\xi_j)^{j-1} (\eta_k)^{k-1}}{1 - \xi_j \eta_k} \right)_{j,k \in \{1, \dots, N\}}. \end{aligned} \quad (8)$$

Plugging Eq. (8) into Eq. (6) and taking the summation $\sum_{y=x}^{\infty} P(y, t)$, we get the following determinantal formula of $F(x, t)$:

$$F(x, t) = \det (K(x, t, j, k))_{j,k \in \{1, \dots, N\}}, \quad (9)$$

where $K(x, t, j, k)$ is defined by $K(x, t, j, k) := -\int_{C_r} d\eta \int_{C_r} d\xi \xi^{x-j-2} \eta^{x-k-2} e^{it(E_\eta - E_\xi)} / (4\pi(1 - \xi\eta))$. This determinantal form of Eq. (9) is compatible with random matrix theory for GUE because many formulae for GUE are given by determinants [16, 60].

Derivation of the GUE Tracy-Widom distribution.– Using Eq. (9), we shall show that $F(x, t)$ converges to the GUE Tracy-Widom distribution function $F_2(\bullet)$ in the long-time limit. A determinant with a function being similar to $K(x, t, j, k)$ was investigated with techniques of Toeplitz operators [62] in Ref. [33]. Following the same techniques with $N \rightarrow \infty$, we obtain

$$F(x, t) = \det (1 - K_B(t, m, n))_{l^2(\{2-x, 3-x, \dots\})} \quad (10)$$

with $K_B(t, m, n) := t (J_m(t) J_{n+1}(t) - J_{m+1}(t) J_n(t)) / (2m - 2n)$. We apply the asymptotic analysis with a scaling variable s defined through $x = 2 + \lfloor -t - s(t/2)^{1/3} \rfloor$, deriving

$$\lim_{t \rightarrow \infty} F(2 + \lfloor -t - s(t/2)^{1/3} \rfloor, t) = F_2(s). \quad (11)$$

Here the GUE Tracy-Widom distribution function is given by $F_2(s) = \text{Det} [1 - K_{\text{Ai}}(x, y)]_{\mathbb{L}^2(s, \infty)}$ with the Airy Kernel $K_{\text{Ai}}(x, y) := (\text{Ai}(x) \text{Ai}'(y) - \text{Ai}'(x) \text{Ai}(y)) / (x - y)$. From Eq. (11) and the relation $P(x, t) = F(x, t) - F(x +$

$1, t)$, we obtain for $t \gg 1$

$$P(2 + \lfloor -t - s(t/2)^{1/3} \rfloor, t) \simeq \left(\frac{2}{t} \right)^{1/3} \frac{F_2(s)}{ds}. \quad (12)$$

Therefore, we analytically prove the emergence of the GUE Tracy-Widom distribution in the quantum spin model that cannot be mapped to a noninteracting fermion Hamiltonian via the Jordan-Wigner transformation [45, 46].

Relation between exact many-body wavefunctions of the folded XXZ model and the XX model.– We explain that the GUE Tracy-Widom distribution in the folded XXZ model is related to a many-body wavefunction of the XX model.

Let us consider the XX model, Hamiltonian of which is defined by $\hat{H}_{\text{XX}} := \sum_{x \in \mathbb{Z}} (\hat{X}_x \hat{X}_{x+1} + \hat{Y}_x \hat{Y}_{x+1})$ [37, 38]. We denote the many-body wavefunction for this model at time t by $\Phi_{\text{XX}}(x_1, \dots, x_N, t)$ with a constraint ($x_j < x_{j+1}$) and assume that the initial state is the domain-wall state, $\Phi_{\text{XX}}(x_1, \dots, x_N, 0) = \prod_{j=1}^N \delta_{x_j, j}$. As explained in Sec. III of SM [53], the exact form of the many-body wavefunction reads

$$\Phi_{\text{XX}}(x_1, \dots, x_N, t) = \int_{C_r} d\xi \det \left(\xi_k^{x_j - k - 1} e^{-iE_{\xi_j} t} \right)_{j,k \in \{1, \dots, N\}}. \quad (13)$$

On the other hand, the exact many-body wavefunction for the folded XXZ mode with the alternating domain-wall initial state is expressed by

$$\Phi(x_1, \dots, x_N, t) = \int_{C_r} d\xi \det \left(\xi_k^{x_j - j - k - 1} e^{-iE_{\xi_j} t} \right)_{j,k \in \{1, \dots, N\}}, \quad (14)$$

which is proved in Sec. II of SM [53].

We find that the many-body wavefunction of Eq. (14) for the folded XXZ model has the determinantal structure similar to that of Eq. (13) for the XX model. As discussed in Ref. [33], the left-most up-spin for the XX model with the domain-wall initial state obeys the GUE Tracy-Widom distribution. Hence, a mathematical origin for the GUE Tracy-Widom distribution in the folded XXZ is close to that for the XX model.

Numerical study for $P(x, t)$ of the XXZ model.– So far, we have analytically studied the folded XXZ model, which is the effective description for the XXZ model with the large anisotropic interaction ($\Delta \gg 1$). Then, it is natural and intriguing to explore the GUE Tracy-Widom distribution in the XXZ model itself from the theoretical viewpoint, and such exploration is important for discussing experimental possibilities of observing our theoretical prediction since the XXZ model has been experimentally studied [30, 31, 63–65]. We here show our numerical study concerning this issue.

The model used in the numerical simulation is the XXZ model with an open boundary condition. The Hamiltonian is defined by $\hat{H}_{\text{XXZ}}^{(\text{open})} :=$

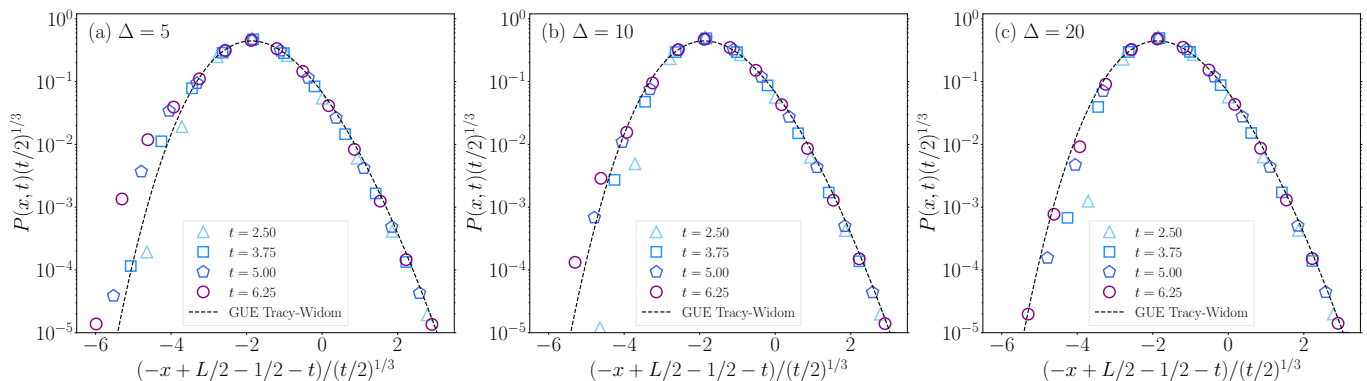


FIG. 2. Numerical results for the probability $P(x, t)$ of finding the left-most up-spin at site x and time t in the XXZ model with the alternating domain-wall initial state. The anisotropic interaction parameter is $\Delta =$ (a) 5, (b) 10, and (c) 20 and the system is $L = 100$. The time evolution of $P(x, t)$ is numerically computed by the TEBD method [47–50]. In order to compare the numerical data with the GUE Tracy-Widom distribution function $F_2(\bullet)$, the ordinate is divided by $(t/2)^{1/3}$ and the abscissas is rescaled by using a result for fast convergence [61], which is described in Sec. IV of SM [53]. The dashed lines in the panels indicates the probability density function $dF_2(s)/ds$ for the GUE Tracy-Widom distribution. The numerical convergences associated with truncation of a matrix product state are discussed in Sec. V of SM [53].

$\sum_{j=1}^{L-1} (\hat{X}_j \hat{X}_{j+1} + \hat{Y}_j \hat{Y}_{j+1} + \Delta \hat{Z}_j \hat{Z}_{j+1})$ with the total number L of the one-dimensional lattice. Here, we assume L to be multiples of four. We denote the quantum state at time t by $|\psi(t)\rangle$ and the initial state is assumed to be the alternating domain-wall state $|\psi(0)\rangle = \prod_{x=L/4}^{L/2} \hat{R}_{2x} |0\rangle$. We numerically solve the Schrödinger equation using the TEBD method [47–50], computing the probability $P(x, t)$ of finding the left-most up-spin at site x and time t .

Figure 2 displays numerical results of $P(x, t)$ with $\Delta = 5, 10$, and 20, where we rescale the abscissas and the ordinates by following Eq. (12) and a result for fast convergence described in Sec. IV of SM [53]. We find that deviations between the numerical data and the probability density function $dF_2(s)/ds$ become large when Δ is small. Thus, we speculate the absence of the GUE Tracy-Widom distribution for the XXZ model in the *long-time limit*.

We, however, find the signature that the probability $P([-t - s(t/2)^{1/3}], t)$ in the right region ($s > 0$) of Fig. 2 exhibits the universal curve being independent of Δ . This curve is characterized by the diagonal Airy kernel $K_{\text{Ai}}(s, s)$ because the dashed line represents the GUE Tracy-Widom distribution (see Sec. VI and Fig. S-4 of SM [53]).

Discussion.— We discuss two topics: (i) the universal behavior of $P(x, t)$ in the XXZ model and (ii) experimental possibilities of observing our theoretical prediction.

As to (i), we discuss the signature that the curve of $P([-t - s(t/2)^{1/3}], t)$ for large $s > 0$ is independent of Δ as pointed out in Fig. 2. We here discuss its origin analytically in the two limiting cases, namely $\Delta = 0$ and large Δ . First we consider the case with $\Delta = 0$. As derived exactly in Sec. VI of SM [53], we have $\lim_{t \rightarrow \infty} F(2 + [-t - s(t/2)^{1/3}], t) = F_{\text{Ai}}(s, 1/2)$

with $F_{\text{Ai}}(s, a) := \text{Det}[1 - aK_{\text{Ai}}(x, y)]_{\mathbb{L}^2(s, \infty)}$. Then, the distribution function approximately is approximately to be $F_{\text{Ai}}(s, 1/2) \simeq 1 - \int_s^\infty dy K_{\text{Ai}}(y, y)/2$ for large s because $K_{\text{Ai}}(x, y)$ is small. Hence, the rescaled probability of finding the left-most up-spin is described by $dF_{\text{Ai}}(s, 1/2)/ds \simeq K_{\text{Ai}}(s, s)/2$ (see Fig. S-4 of SM [53]). Second, we consider the folded XXZ model corresponding to large Δ . Using Eq. (11), we similarly approximate the probability distribution function as $F_2(s) \simeq 1 - \int_s^\infty dy K_{\text{Ai}}(y, y)$ for large s , obtaining that the rescaled probability is characterized by $K_{\text{Ai}}(s, s)$. Combing our analytical discussions and the numerical findings of Fig. 2, we find the signature that the probability of finding the left-most up-spin for large s is universally characterized by the diagonal Airy kernel $K_{\text{Ai}}(s, s)$ regardless of Δ . Finally, we mention that the conjecture by Saenz, Tracy, and Widom for the XXZ model (see Conjecture 1 of Ref. [33]) may be useful for proving the diagonal Airy kernel in the dynamics of the XXZ model (see Sec. VII of SM [53]).

As to (ii) we discuss experimental possibilities of observing the GUE Tracy-Widom distribution function in quantum spin transport on one-dimensional systems. As shown in Fig. 2, the probability $P(x, t)$ in the XXZ model with $\Delta \gg 1$ shows the signature of the GUE Tracy-Widom behavior in the *finite time regions*, and its time scale is about 5 times spin flipping. On the experimental side, previous literature in cold atom experiments [30, 63–65] realized the XXZ model as an effective description for a two-component Bose-Hubbard model under the hard-core limit [66–68], and also an experiment using superconducting qubits [31] simulates the XXZ model by periodical applications of 2-qubit unitary gates. These experiments accessed the spin transport where the spins flip more than 5 times. Taking these

experimental achievements into account, we expect that signatures of the GUE Tracy-Widom distribution may be observed in state-of-the-art experiments.

Conclusions and future prospects.— We theoretically studied the one-dimensional quantum spin transport described by the folded XXZ model with the alternating domain-wall initial state by focusing on the probability $P(x, t)$ of finding the left-most up-spin. Employing the exact method based on the Bethe ansatz, we exactly demonstrated that the rescaled probability converges to the probability density function for the GUE Tracy-Widom distribution function in the long-time limit. Beyond the folded XXZ model, we numerically studied the XXZ model via the TEBD method, discussing the universal behavior in terms of the diagonal Airy Kernel.

As a future prospect, it is interesting to explore the Tracy-Widom distribution in the quantum transport of non-integrable models. So far, the GUE Tracy-Widom distribution in quantum transport has been investigated in integrable models, and thus it is intriguing to uncover the role of the integrability and understand how universal the Tracy-Widom distribution is in quantum transport.

Also, studying the Tracy-Widom distribution in other integral models is interesting. One of such examples is a phase model. This model describes strongly interacting bosons on a one-dimensional lattice [69–71] and have scattering amplitudes being similar to the folded XXZ model. As another prospect, it is fundamentally important to understand the universal behavior of the XXZ model analytically by using the generalized hydrodynamics [34, 72–86] and ballistic macroscopic fluctuation theory [87, 88].

ACKNOWLEDGMENTS

KF and ST are grateful to Ryusuke Hamazaki and Yuki Kawaguchi for the valuable comments on the manuscript, and Ipei Danshita for the helpful comments on experiments of ultracold atoms. The work of KF has been supported by JSPS KAKENHI Grant No. JP23K13029. The work of TS has been supported by JSPS KAKENHI Grants No. JP21H04432, No. JP22H01143.

-
- [1] A. Dhar, Heat transport in low-dimensional systems, *Advances in Physics* **57**, 457 (2008).
 - [2] N. Nagaosa, J. Sinova, S. Onoda, A. H. MacDonald, and N. P. Ong, Anomalous hall effect, *Rev. Mod. Phys.* **82**, 1539 (2010).
 - [3] M. C. Marchetti, J. F. Joanny, S. Ramaswamy, T. B. Liverpool, J. Prost, M. Rao, and R. A. Simha, Hydrodynamics of soft active matter, *Rev. Mod. Phys.* **85**, 1143 (2013).
 - [4] B. Bertini, F. Heidrich-Meisner, C. Karrasch, T. Prosen, R. Steinigeweg, and M. Žnidarič, Finite-temperature transport in one-dimensional quantum lattice models, *Rev. Mod. Phys.* **93**, 025003 (2021).
 - [5] T. Sasamoto, Fluctuations of the one-dimensional asymmetric exclusion process using random matrix techniques, *Journal of Statistical Mechanics: Theory and Experiment* **2007**, P07007 (2007).
 - [6] T. Kriecherbauer and J. Krug, A pedestrian’s view on interacting particle systems, KPZ universality and random matrices, *Journal of Physics A: Mathematical and Theoretical* **43**, 403001 (2010).
 - [7] I. Corwin, The Kardar-Parisi-Zhang equation and universality class, *Random Matrices: Theory and Applications* **01**, 1130001 (2012).
 - [8] J. Quastel and H. Spohn, The one-dimensional KPZ equation and its universality class, *Journal of Statistical Physics* **160**, 965 (2015).
 - [9] K. A. Takeuchi, An appetizer to modern developments on the Kardar-Parisi-Zhang universality class, *Physica A: Statistical Mechanics and its Applications* **504**, 77 (2018), lecture Notes of the 14th International Summer School on Fundamental Problems in Statistical Physics.
 - [10] A.-L. Barabási and H. E. Stanley, *Fractal concepts in surface growth* (Cambridge university press, 1995).
 - [11] B. Schmittmann and R. Zia, Statistical mechanics of driven diffusive systems, in *Statistical Mechanics of Driven Diffusive System*, Phase Transitions and Critical Phenomena, Vol. 17, edited by B. Schmittmann and R. Zia (Academic Press, 1995) pp. 3–214.
 - [12] T. M. Liggett, *Stochastic interacting systems: contact, voter and exclusion processes*, Vol. 324 (springer science & Business Media, 2013).
 - [13] C. A. Tracy and H. Widom, Level-spacing distributions and the Airy kernel, *Physics Letters B* **305**, 115 (1993).
 - [14] C. A. Tracy and H. Widom, On orthogonal and symplectic matrix ensembles, *Communications in Mathematical Physics* **177**, 727 (1996).
 - [15] P. Forrester, The spectrum edge of random matrix ensembles, *Nuclear Physics B* **402**, 709 (1993).
 - [16] P. J. Forrester, *Log-gases and random matrices (LMS-34)* (Princeton university press, 2010).
 - [17] A. Nahum, J. Ruhman, S. Vijay, and J. Haah, Quantum entanglement growth under random unitary dynamics, *Phys. Rev. X* **7**, 031016 (2017).
 - [18] M. Ljubotina, M. Žnidarič, and T. Prosen, Kardar-Parisi-Zhang physics in the quantum Heisenberg magnet, *Phys. Rev. Lett.* **122**, 210602 (2019).
 - [19] M. Dupont and J. E. Moore, Universal spin dynamics in infinite-temperature one-dimensional quantum magnets, *Phys. Rev. B* **101**, 121106 (2020).
 - [20] J. De Nardis, S. Gopalakrishnan, E. Ilievski, and R. Vasseur, Superdiffusion from emergent classical solitons in quantum spin chains, *Phys. Rev. Lett.* **125**, 070601 (2020).
 - [21] K. Fujimoto, R. Hamazaki, and Y. Kawaguchi, Family-vicek scaling of roughness growth in a strongly interacting bose gas, *Phys. Rev. Lett.* **124**, 210604 (2020).
 - [22] B. Ye, F. Machado, J. Kemp, R. B. Hutson, and N. Y. Yao, Universal Kardar-Parisi-Zhang dynamics in integrable quantum systems, *Phys. Rev. Lett.* **129**, 230602 (2022).

- (2022).
- [23] C. P. Moca, M. A. Werner, A. Valli, T. Prosen, and G. Zaránd, Kardar-Parisi-Zhang scaling in the hubbard model, *Phys. Rev. B* **108**, 235139 (2023).
- [24] J. De Nardis, S. Gopalakrishnan, and R. Vasseur, Nonlinear fluctuating hydrodynamics for Kardar-Parisi-Zhang scaling in isotropic spin chains, *Phys. Rev. Lett.* **131**, 197102 (2023).
- [25] S. Mu, J. Gong, and G. Lemarié, Kardar-Parisi-Zhang physics in the density fluctuations of localized two-dimensional wave packets, *Phys. Rev. Lett.* **132**, 046301 (2024).
- [26] G. Cecile, J. De Nardis, and E. Ilievski, Squeezed ensembles and anomalous dynamic roughening in interacting integrable chains, *Phys. Rev. Lett.* **132**, 130401 (2024).
- [27] S. Gopalakrishnan and R. Vasseur, Superdiffusion from nonabelian symmetries in nearly integrable systems, *Annual Review of Condensed Matter Physics* **15**, 159 (2024).
- [28] S. Aditya and N. Roy, Family-vicsek dynamical scaling and Kardar-Parisi-Zhang-like superdiffusive growth of surface roughness in a driven one-dimensional quasiperiodic model, *Phys. Rev. B* **109**, 035164 (2024).
- [29] A. Scheie, N. E. Sherman, M. Dupont, S. E. Nagler, M. B. Stone, G. E. Granroth, J. E. Moore, and D. A. Tennant, Detection of Kardar-Parisi-Zhang hydrodynamics in a quantum Heisenberg spin-1/2 chain, *Nature Physics* **17**, 726 (2021).
- [30] D. Wei, A. Rubio-Abadal, B. Ye, F. Machado, J. Kemp, K. Srakaew, S. Hollerith, J. Rui, S. Gopalakrishnan, N. Y. Yao, I. Bloch, and J. Zeiher, Quantum gas microscopy of Kardar-Parisi-Zhang superdiffusion, *Science* **376**, 716 (2022).
- [31] E. Rosenberg, T. I. Andersen, R. Samajdar, A. Petukhov, J. C. Hoke, D. Abanin, A. Bengtsson, I. K. Drozdov, C. Erickson, P. V. Klimov, X. Mi, A. Morvan, M. Neeley, C. Neill, R. Acharya, R. Allen, K. Anderson, M. Ansmann, F. Arute, K. Arya, A. Asfaw, J. Atalaya, J. C. Bardin, A. Bilmes, G. Bortoli, A. Bourassa, J. Bovaird, L. Brill, M. Broughton, B. B. Buckley, D. A. Buell, T. Burger, B. Burkett, N. Bushnell, J. Campero, H.-S. Chang, Z. Chen, B. Chiaro, D. Chik, J. Cogan, R. Collins, P. Conner, W. Courtney, A. L. Crook, B. Curtin, D. M. Debroy, A. D. T. Barba, S. Demura, A. D. Paolo, A. Dunsworth, C. Earle, L. Faoro, E. Farhi, R. Fatemi, V. S. Ferreira, L. F. Burgos, E. Forati, A. G. Fowler, B. Foxen, G. Garcia, É. Genois, W. Jiang, C. Gidney, D. Gilboa, M. Giustina, R. Gosula, A. G. Dau, J. A. Gross, S. Habegger, M. C. Hamilton, M. Hansen, M. P. Harrigan, S. D. Harrington, P. Heu, G. Hill, M. R. Hoffmann, S. Hong, T. Huang, A. Huff, W. J. Huggins, L. B. Ioffe, S. V. Isakov, J. Iveland, E. Jeffrey, Z. Jiang, C. Jones, P. Juhas, D. Kafri, T. Khatyar, M. Khezri, M. Kieferová, S. Kim, A. Kitaev, A. R. Klots, A. N. Korotkov, F. Kostritsa, J. M. Kreikebaum, D. Landhuis, P. Laptev, K.-M. Lau, L. Laws, J. Lee, K. W. Lee, Y. D. Lensky, B. J. Lester, A. T. Lill, W. Liu, A. Locharla, S. Mandrà, O. Martin, S. Martin, J. R. McClean, M. McEwen, S. Meeks, K. C. Miao, A. Mieszala, S. Montazeri, R. Movassagh, W. Mruczkiewicz, A. Nersisyan, M. Newman, J. H. Ng, A. Nguyen, M. Nguyen, M. Y. Niu, T. E. O'Brien, S. Omonije, A. Opremcak, R. Potter, L. P. Pryadko, C. Quintana, D. M. Rhodes, C. Rocque, N. C. Rubin, N. Saei, D. Sank, K. Sankaragomathi, K. J. Satzinger, H. F. Schurkus, C. Schuster, M. J. Shearn, A. Shorter, N. Shutty, V. Shvarts, V. Sivak, J. Skrzynny, W. C. Smith, R. D. Somma, G. Sterling, D. Strain, M. Szalay, D. Thor, A. Torres, G. Vidal, B. Villalonga, C. V. Heidweiller, T. White, B. W. K. Woo, C. Xing, Z. J. Yao, P. Yeh, J. Yoo, G. Young, A. Zalcman, Y. Zhang, N. Zhu, N. Zobrist, H. Neven, R. Babbush, D. Bacon, S. Boixo, J. Hilton, E. Lucero, A. Megrant, J. Kelly, Y. Chen, V. Smelyanskiy, V. Khemani, S. Gopalakrishnan, T. Prosen, and P. Roushan, Dynamics of magnetization at infinite temperature in a Heisenberg spin chain, *Science* **384**, 48 (2024).
- [32] V. Eisler and Z. Rácz, Full counting statistics in a propagating quantum front and random matrix spectra, *Phys. Rev. Lett.* **110**, 060602 (2013).
- [33] A. Saenz, C. A. Tracy, and H. Widom, Domain Walls in the Heisenberg-Ising Spin-1/2 Chain, in *Toeplitz Operators and Random Matrices: In Memory of Harold Widom*, edited by E. Basor, A. Böttcher, T. Ehrhardt, and C. A. Tracy (Springer International Publishing, Cham, 2022) pp. 9–47.
- [34] M. Collura, A. De Luca, and J. Viti, Analytic solution of the domain-wall nonequilibrium stationary state, *Phys. Rev. B* **97**, 081111 (2018).
- [35] J.-M. Stéphan, Free fermions at the edge of interacting systems, *SciPost Phys.* **6**, 057 (2019).
- [36] V. B. Bulchandani and C. Karrasch, Subdiffusive front scaling in interacting integrable models, *Phys. Rev. B* **99**, 121410 (2019).
- [37] M. Takahashi, Thermodynamics of one-dimensional solvable models, (1999).
- [38] F. Franchini *et al.*, *An introduction to integrable techniques for one-dimensional quantum systems*, Vol. 940 (Springer, 2017).
- [39] Z.-C. Yang, F. Liu, A. V. Gorshkov, and T. Iadecola, Hilbert-space fragmentation from strict confinement, *Phys. Rev. Lett.* **124**, 207602 (2020).
- [40] L. Zadnik and M. Fagotti, The Folded Spin-1/2 XXZ Model: I. Diagonalisation, Jamming, and Ground State Properties, *SciPost Phys. Core* **4**, 010 (2021).
- [41] L. Zadnik, K. Bidzhev, and M. Fagotti, The folded spin-1/2 XXZ model: II. Thermodynamics and hydrodynamics with a minimal set of charges, *SciPost Phys.* **10**, 099 (2021).
- [42] B. Pozsgay, T. Gombor, A. Hutsalyuk, Y. Jiang, L. Pristyák, and E. Vernier, Integrable spin chain with Hilbert space fragmentation and solvable real-time dynamics, *Phys. Rev. E* **104**, 044106 (2021).
- [43] B. Pozsgay, T. Gombor, and A. Hutsalyuk, Integrable hard-rod deformation of the Heisenberg spin chains, *Phys. Rev. E* **104**, 064124 (2021).
- [44] M. Borsi, L. Pristyák, and B. Pozsgay, Matrix product symmetries and breakdown of thermalization from hard rod deformations, *Phys. Rev. Lett.* **131**, 037101 (2023).
- [45] S. Sachdev, Quantum phase transitions, *Physics world* **12**, 33 (1999).
- [46] M. Lewenstein, A. Sanpera, and V. Ahufinger, *Ultracold Atoms in Optical Lattices: Simulating quantum many-body systems* (Oxford University Press, 2012).
- [47] G. Vidal, Efficient classical simulation of slightly entangled quantum computations, *Phys. Rev. Lett.* **91**, 147902 (2003).
- [48] G. Vidal, Efficient simulation of one-dimensional quantum many-body systems, *Phys. Rev. Lett.* **93**, 040502 (2004).

- [49] U. Schollwöck, The density-matrix renormalization group in the age of matrix product states, *Annals of Physics* **326**, 96 (2011).
- [50] S. Paeckel, T. Köhler, A. Swoboda, S. R. Manmana, U. Schollwöck, and C. Hubig, Time-evolution methods for matrix-product states, *Annals of Physics* **411**, 167998 (2019).
- [51] G. M. Schütz, Exact solution of the master equation for the asymmetric exclusion process, *Journal of Statistical Physics* **88**, 427 (1997).
- [52] C. A. Tracy and H. Widom, Integral formulas for the asymmetric simple exclusion process, *Communications in Mathematical Physics* **279**, 815 (2008).
- [53] See Supplemental Material for (I) Proof of Eq. (5) in the main text, (II) Determinantal formula for Eq. (5) in the main text, (III) Proof of Eq. (13) in the main text, (IV) Asymptotic analysis to the GUE Tracy-Widom distribution with fast convergence, (V) Numerical truncation in the TEBD method, (VI) Limiting probability distribution function for $\Delta = 0$, and (VII) Conjecture for the XXZ model by Saenz, Tracy, and Widom.
- [54] L. Cantini, F. Colomo, and A. G. Pronko, Integral formulas and antisymmetrization relations for the six-vertex model, *Annales Henri Poincaré* **21**, 865 (2020).
- [55] L. Petrov, Refined Cauchy identity for spin Hall-Littlewood symmetric rational functions, *Journal of Combinatorial Theory, Series A* **184**, 105519 (2021).
- [56] V. E. Korepin, Calculation of norms of Bethe wave functions, *Communications in Mathematical Physics* **86**, 391 (1982).
- [57] A. G. Izergin, Partition function of the six-vertex model in a finite volume, *Soviet Physics Doklady* **32**, 878 (1987).
- [58] A. G. Izergin, D. A. Coker, and V. E. Korepin, Determinant formula for the six-vertex model, *Journal of Physics A: Mathematical and General* **25**, 4315 (1992).
- [59] V. E. Korepin, N. M. Bogoliubov, and A. G. Izergin, *Quantum Inverse Scattering Method and Correlation Functions*, Cambridge Monographs on Mathematical Physics (Cambridge University Press, 1993).
- [60] M. L. Mehta, *Random matrices* (Elsevier, 2004).
- [61] P. L. Ferrari and R. Frings, Finite time corrections in KPZ growth models, *Journal of Statistical Physics* **144**, 1123 (2011).
- [62] A. Böttcher and B. Silbermann, *Introduction to large truncated Toeplitz matrices* (Springer Science & Business Media, 2012).
- [63] P. N. Jepsen, J. Amato-Grill, I. Dimitrova, W. W. Ho, E. Demler, and W. Ketterle, Spin transport in a tunable heisenberg model realized with ultracold atoms, *Nature* **588**, 403 (2020).
- [64] P. N. Jepsen, W. W. Ho, J. Amato-Grill, I. Dimitrova, E. Demler, and W. Ketterle, Transverse spin dynamics in the anisotropic heisenberg model realized with ultracold atoms, *Phys. Rev. X* **11**, 041054 (2021).
- [65] P. N. Jepsen, Y. K. E. Lee, H. Lin, I. Dimitrova, Y. Margalit, W. W. Ho, and W. Ketterle, Long-lived phantom helix states in Heisenberg quantum magnets, *Nature Physics* **18**, 899 (2022).
- [66] E. Altman, W. Hofstetter, E. Demler, and M. D. Lukin, Phase diagram of two-component bosons on an optical lattice, *New Journal of Physics* **5**, 113 (2003).
- [67] L.-M. Duan, E. Demler, and M. D. Lukin, Controlling spin exchange interactions of ultracold atoms in optical lattices, *Phys. Rev. Lett.* **91**, 090402 (2003).
- [68] A. B. Kuklov and B. V. Svistunov, Counterflow superfluidity of two-species ultracold atoms in a commensurate optical lattice, *Phys. Rev. Lett.* **90**, 100401 (2003).
- [69] N. M. Bogoliubov, R. K. Bullough, and G. D. Pang, Exact solution of a q-boson hopping model, *Phys. Rev. B* **47**, 11495 (1993).
- [70] N. Bogoliubov, A. Izergin, and N. Kitanine, Correlation functions for a strongly correlated boson system, *Nuclear Physics B* **516**, 501 (1998).
- [71] B. Pozsgay and V. Eisler, Real-time dynamics in a strongly interacting bosonic hopping model: global quenches and mapping to the XX chain, *Journal of Statistical Mechanics: Theory and Experiment* **2016**, 053107 (2016).
- [72] O. A. Castro-Alvaredo, B. Doyon, and T. Yoshimura, Emergent hydrodynamics in integrable quantum systems out of equilibrium, *Phys. Rev. X* **6**, 041065 (2016).
- [73] B. Bertini, M. Collura, J. De Nardis, and M. Fagotti, Transport in out-of-equilibrium XXZ chains: Exact profiles of charges and currents, *Phys. Rev. Lett.* **117**, 207201 (2016).
- [74] B. Doyon and T. Yoshimura, A note on generalized hydrodynamics: inhomogeneous fields and other concepts, *SciPost Phys.* **2**, 014 (2017).
- [75] B. Doyon, J. Dubail, R. Konik, and T. Yoshimura, Large-scale description of interacting one-dimensional bose gases: Generalized hydrodynamics supersedes conventional hydrodynamics, *Phys. Rev. Lett.* **119**, 195301 (2017).
- [76] V. B. Bulchandani, R. Vasseur, C. Karrasch, and J. E. Moore, Solvable hydrodynamics of quantum integrable systems, *Phys. Rev. Lett.* **119**, 220604 (2017).
- [77] V. B. Bulchandani, R. Vasseur, C. Karrasch, and J. E. Moore, Bethe-boltzmann hydrodynamics and spin transport in the XXZ chain, *Phys. Rev. B* **97**, 045407 (2018).
- [78] B. Doyon, T. Yoshimura, and J.-S. Caux, Soliton gases and generalized hydrodynamics, *Phys. Rev. Lett.* **120**, 045301 (2018).
- [79] J. De Nardis, D. Bernard, and B. Doyon, Hydrodynamic diffusion in integrable systems, *Phys. Rev. Lett.* **121**, 160603 (2018).
- [80] S. Gopalakrishnan and R. Vasseur, Kinetic theory of spin diffusion and superdiffusion in XXZ spin chains, *Phys. Rev. Lett.* **122**, 127202 (2019).
- [81] M. Schemmer, I. Bouchoule, B. Doyon, and J. Dubail, Generalized hydrodynamics on an atom chip, *Phys. Rev. Lett.* **122**, 090601 (2019).
- [82] B. Doyon, Lecture notes on Generalised Hydrodynamics, *SciPost Phys. Lect. Notes*, 18 (2020).
- [83] V. Alba, B. Bertini, M. Fagotti, L. Piroli, and P. Ruggiero, Generalized-hydrodynamic approach to inhomogeneous quenches: correlations, entanglement and quantum effects, *Journal of Statistical Mechanics: Theory and Experiment* **2021**, 114004 (2021).
- [84] N. Malvania, Y. Zhang, Y. Le, J. Dubail, M. Rigol, and D. S. Weiss, Generalized hydrodynamics in strongly interacting 1d bose gases, *Science* **373**, 1129 (2021).
- [85] I. Bouchoule and J. Dubail, Generalized hydrodynamics in the one-dimensional bose gas: theory and experiments, *Journal of Statistical Mechanics: Theory and Experiment* **2022**, 014003 (2022).
- [86] F. H. Essler, A short introduction to generalized hydrodynamics, *Physica A: Statistical Mechanics and its Applications* **631**, 127572 (2023), lecture Notes of the 15th

International Summer School of Fundamental Problems
in Statistical Physics.

- [87] B. Doyon, G. Perfetto, T. Sasamoto, and T. Yoshimura, Emergence of hydrodynamic spatial long-range correlations in nonequilibrium many-body systems, [Phys. Rev. Lett.](#) **131**, 027101 (2023).
- [88] B. Doyon, G. Perfetto, T. Sasamoto, and T. Yoshimura, Ballistic macroscopic fluctuation theory, [SciPost Phys.](#) **15**, 136 (2023).
- [89] F. Bornemann, On the numerical evaluation of distributions in random matrix theory: A review, [Markov Proc. Relat. Fields](#) **16**, 803 (2010).

**SUPPLEMENTAL MATERIAL FOR “QUANTUM TRANSPORT IN INTERACTING SPIN CHAINS:
EXACT DERIVATION OF THE GUE TRACY-WIDOM DISTRIBUTION”**

Kazuya Fujimoto and Tomohiro Sasamoto

Department of Physics, Institute of Science Tokyo, 2-12-1 Ookayama, Meguro-ku, Tokyo 152-8551, Japan

This Supplemental Material describes the following:

- (I) Proof of Eq. (5) in the main text,
- (II) Determinantal formula for Eq. (5) in the main text,
- (III) Proof of Eq. (13) in the main text,
- (IV) Asymptotic analysis to the GUE Tracy-Widom ditribution with fast convergence,
- (V) Numerical truncation in the TEBD method,
- (VI) Limiting probability distribution function for $\Delta = 0$,
- (VII) Conjecture for the XXZ model by Saenz, Tracy, and Widom.

I. PROOF OF EQ. (5) IN THE MAIN TEXT

We prove that Eq. (5) in the main text satisfies the Schrödinger equation with \hat{H}_{fXXZ} and the initial state $|\phi(0)\rangle = \prod_{j=1}^N \hat{R}_{y_j} |0\rangle$ with the constraint $y_j + 2 \leq y_{j+1}$. Here, y_j indicates the initial up-spin site label. Note that the many-body wavefunction $\Phi(x_1, \dots, x_N, t)$ under this setting becomes zero if the condition $x_j + 2 \leq x_{j+1}$ does not hold, because all the matrix elements of \hat{H}_{fXXZ} for breaking this condition is zero. Hence, in the following, we consider $\Phi(x_1, \dots, x_N, t)$ under the restricted configuration $x_j + 2 \leq x_{j+1}$.

We first derive equations that $\Phi(x_1, \dots, x_N, t)$ satisfies. From the Schrödinger equation for the folded XXZ model, we obtain the equation of motion as

$$i \frac{\partial}{\partial t} \Phi(x_1, \dots, x_N, t) = \frac{1}{2} \sum_{j=1}^N \left(\underbrace{\Phi(x_1, \dots, x_j + 1, \dots, x_N, t)}_j + \underbrace{\Phi(x_1, \dots, x_j - 1, \dots, x_N, t)}_j \right) \quad (\text{S-1})$$

with the boundary condition defined by

$$\underbrace{\Phi(x_1, \dots, x_j + 1, x_j + 2, \dots, x_N, t)}_j + \underbrace{\Phi(x_1, \dots, x_j, x_j + 1, \dots, x_N, t)}_{j+1} = 0. \quad (\text{S-2})$$

Here, the boundary condition comes from the fact that breaking the condition $x_j + 2 \leq x_{j+1}$ leads to $\Phi(x_1, \dots, x_N, t) = 0$. The initial state considered here becomes

$$\Phi(x_1, \dots, x_N, 0) = \prod_{j=1}^N \delta_{x_j, y_j}, \quad (\text{S-3})$$

Under this setup, the exact many-body wavefunction is given by

$$\Phi(x_1, \dots, x_N, t) = \int_{C_r} d\xi \sum_{\sigma \in \mathbb{S}_N} A_\sigma(\xi) \prod_{j=1}^N \xi_{\sigma_j}^{x_j - y_{\sigma_j} - 1} e^{-iE_{\xi_j} t}. \quad (\text{S-4})$$

In the following subsections, we prove that Eq. (S-4) solves Eqs. (S-1), (S-2), and (S-3).

A. Proof for Eq. (S-4) satisfying the equation (S-1) of motion

We substitute Eq. (S-4) into Eq. (S-1), obtaining

$$\text{LHS of Eq. (S-1)} = \int_{C_r} d\xi \sum_{\sigma \in \mathbb{S}_N} A_\sigma(\xi) \left(\sum_{k=1}^N E_{\xi_k} \right) \left(\prod_{j=1}^N \xi_{\sigma_j}^{x_j - y_{\sigma_j} - 1} e^{-iE_{\xi_j} t} \right), \quad (\text{S-5})$$

$$\text{RHS of Eq. (S-1)} = \frac{1}{2} \sum_{k=1}^N \int_{C_r} d\xi \sum_{\sigma \in \mathbb{S}_N} A_\sigma(\xi) (\xi_{\sigma_k} + \xi_{\sigma_k}^{-1}) \left(\prod_{j=1}^N \xi_{\sigma_j}^{x_j - y_{\sigma_j} - 1} e^{-iE_{\xi_j} t} \right) \quad (\text{S-6})$$

$$= \int_{C_r} d\xi \sum_{\sigma \in \mathbb{S}_N} A_\sigma(\xi) \left\{ \frac{1}{2} \sum_{k=1}^N (\xi_{\sigma_k} + \xi_{\sigma_k}^{-1}) \right\} \left(\prod_{j=1}^N \xi_{\sigma_j}^{x_j - y_{\sigma_j} - 1} e^{-iE_{\xi_j} t} \right) \quad (\text{S-7})$$

$$= \int_{C_r} d\xi \sum_{\sigma \in \mathbb{S}_N} A_\sigma(\xi) \left\{ \frac{1}{2} \sum_{k=1}^N (\xi_k + \xi_k^{-1}) \right\} \left(\prod_{j=1}^N \xi_{\sigma_j}^{x_j - y_{\sigma_j} - 1} e^{-iE_{\xi_j} t} \right) \quad (\text{S-8})$$

$$= \int_{C_r} d\xi \sum_{\sigma \in \mathbb{S}_N} A_\sigma(\xi) \left(\sum_{k=1}^N E_{\xi_k} \right) \left(\prod_{j=1}^N \xi_{\sigma_j}^{x_j - y_{\sigma_j} - 1} e^{-iE_{\xi_j} t} \right). \quad (\text{S-9})$$

Here, we use the formula $\sum_{k=1}^N f(\xi_{\sigma_k}) = \sum_{k=1}^N f(\xi_k)$ with a function $f(\bullet)$ to get Eq. (S-8). Comparing Eq. (S-5) with Eq. (S-9), we complete the proof.

B. Proof for Eq. (S-4) satisfying the boundary condition of Eq. (S-2)

We substitute Eq. (S-4) into Eq. (S-2), obtaining

$$\text{LHS of Eq. (S-2)} \quad (\text{S-10})$$

$$= \int_{C_r} d\xi \sum_{\sigma \in \mathbb{S}_N} A_\sigma(\xi) \left(\prod_{l \in \{1, \dots, N\}: l \neq j, j+1} \xi_{\sigma_l}^{x_l - y_{\sigma_l} - 1} e^{-iE_{\xi_l} t} \right) e^{-i(E_{\xi_j} + E_{\xi_{j+1}})t} \left(\xi_{\sigma_j}^{x_j - y_{\sigma_j}} \xi_{\sigma_{j+1}}^{x_j - y_{\sigma_{j+1}} + 1} + \xi_{\sigma_j}^{x_j - y_{\sigma_j} - 1} \xi_{\sigma_{j+1}}^{x_j - y_{\sigma_{j+1}}} \right) \quad (\text{S-11})$$

$$= \int_{C_r} d\xi \sum_{\sigma \in \mathbb{S}_N} A_\sigma(\xi) \left(\prod_{l \in \{1, \dots, N\}: l \neq j, j+1} \xi_{\sigma_l}^{x_l - y_{\sigma_l} - 1} e^{-iE_{\xi_l} t} \right) e^{-i(E_{\xi_j} + E_{\xi_{j+1}})t} \xi_{\sigma_j}^{x_j - y_{\sigma_j}} \xi_{\sigma_{j+1}}^{x_j - y_{\sigma_{j+1}}} (\xi_{\sigma_{j+1}} + \xi_{\sigma_j}^{-1}) \quad (\text{S-12})$$

$$= \int_{C_r} d\xi \sum_{\sigma \in \mathbb{S}_N} G_\sigma(\xi, j). \quad (\text{S-13})$$

Here, we define the function $G_\sigma(\xi, j)$ as

$$G_\sigma(\xi, j) := A_\sigma(\xi) \left(\prod_{l \in \{1, \dots, N\}: l \neq j, j+1} \xi_{\sigma_l}^{x_l - y_{\sigma_l} - 1} e^{-iE_{\xi_l} t} \right) e^{-i(E_{\xi_j} + E_{\xi_{j+1}})t} \xi_{\sigma_j}^{x_j - y_{\sigma_j}} \xi_{\sigma_{j+1}}^{x_j - y_{\sigma_{j+1}}} (\xi_{\sigma_{j+1}} + \xi_{\sigma_j}^{-1}). \quad (\text{S-14})$$

Next, for a fixed permutation σ , we consider a new permutation μ defined by

$$\mu_l := \begin{cases} \sigma_l & (l \neq j, j+1) \\ \sigma_j & (l = j+1) \\ \sigma_{j+1} & (l = j) \end{cases} \quad (\text{S-15})$$

Then, by definition, we can show

$$A_\mu(\xi) = A_\sigma(\xi) S(\xi_{\sigma_{j+1}}, \xi_{\sigma_j}). \quad (\text{S-16})$$

Using Eqs. (S-14) and (S-16), we can prove

$$G_\sigma(\xi, j) + G_\mu(\xi, j) \quad (\text{S-17})$$

$$= A_\sigma(\xi) \left(\prod_{l \in \{1, \dots, N\}: l \neq j, j+1} \xi_{\sigma_l}^{x_l - y_{\sigma_l} - 1} e^{-iE_{\xi_l} t} \right) e^{-i(E_{\xi_j} + E_{\xi_{j+1}})t} \xi_{\sigma_j}^{x_j - y_{\sigma_j}} \xi_{\sigma_{j+1}}^{x_j - y_{\sigma_{j+1}}} \left\{ \xi_{\sigma_{j+1}} + \xi_{\sigma_j}^{-1} - \frac{\xi_{\sigma_{j+1}}}{\xi_{\sigma_j}} (\xi_{\sigma_{j+1}}^{-1} + \xi_{\sigma_j}) \right\} \quad (\text{S-18})$$

$$= 0. \tag{S-19}$$

This completes the proof.

C. Proof for Eq. (S-4) satisfying the initial state of Eq. (S-3)

We shall prove that Eq. (S-4) with $t = 0$ leads to Eq. (S-3). First, we derive the explicit expression of $A_\sigma(\boldsymbol{\xi})$ in Eq. (S-4) by introducing three sets $U := \{1, \dots, N\}$, $P := \{(\alpha, \beta) | \alpha < \beta \wedge \alpha, \beta \in U\}$, $P_\sigma^< := \{(\alpha, \beta) | \sigma_\alpha < \sigma_\beta \wedge (\alpha, \beta) \in P\}$, and $P_\sigma^> := \{(\alpha, \beta) | \sigma_\alpha > \sigma_\beta \wedge (\alpha, \beta) \in P\}$. Then, we can derive

$$A_\sigma(\boldsymbol{\xi}) = \text{sgn}(\sigma) \prod_{(\alpha, \beta) \in P_\sigma^>} \xi_{\sigma_\alpha} \xi_{\sigma_\beta}^{-1} \tag{S-20}$$

$$= \text{sgn}(\sigma) \left(\prod_{(\alpha, \beta) \in P_\sigma^>} \xi_{\sigma_\alpha} \xi_{\sigma_\beta}^{-1} \right) \left(\prod_{(\alpha, \beta) \in P_\sigma^<} \xi_{\sigma_\alpha} \xi_{\sigma_\alpha}^{-1} \right) \tag{S-21}$$

$$= \text{sgn}(\sigma) \left(\prod_{(\alpha, \beta) \in P} \xi_{\sigma_\alpha} \right) \left(\prod_{(\alpha, \beta) \in P} \xi_\alpha^{-1} \right) \tag{S-22}$$

$$= \text{sgn}(\sigma) \prod_{j=1}^N \xi_{\sigma_j}^{\sigma_j - j}. \tag{S-23}$$

We substitute Eq. (S-23) into (S-4), getting

$$\Phi(x_1, \dots, x_N, 0) = \sum_{\sigma \in \mathbb{S}_N} \text{sgn}(\sigma) \int d\boldsymbol{\xi} \prod_{j=1}^N \xi_{\sigma_j}^{x_j - j - y_{\sigma_j} + \sigma_j - 1} \tag{S-24}$$

$$= \sum_{\sigma \in \mathbb{S}_N} \text{sgn}(\sigma) \prod_{j=1}^N \delta_{x_j, y_{\sigma_j} + j - \sigma_j} \tag{S-25}$$

$$= \prod_{j=1}^N \delta_{x_j, y_j}. \tag{S-26}$$

Here, the equality of Eq. (S-26) can be proved by noting that the inequalities $x_j + 2 \leq x_{j+1}$ and $y_j + 2 \leq y_{j+1}$ are violated when there are inversions in σ . In order to show this fact, let us consider integers m and n such that two conditions $m < n$ and $\sigma_m > \sigma_n$ hold. In our setup, we have inequalities $x_n - x_m \geq 2(n - m)$ and $y_{\sigma_m} - y_{\sigma_n} \geq 2(\sigma_m - \sigma_n)$, which can be derived by the above inequalities $x_j + 2 \leq x_{j+1}$ and $y_j + 2 \leq y_{j+1}$. Using a relation $x_j = y_{\sigma_j} + j - \sigma_j$ coming from Eq. (S-25), we can derive

$$x_n - x_m - 2(n - m) = y_{\sigma_n} - y_{\sigma_m} - (n - m) + \sigma_m - \sigma_n \tag{S-27}$$

$$\leq \underbrace{(m - n)}_{<0} + \underbrace{(\sigma_n - \sigma_m)}_{<0}. \tag{S-28}$$

Thus, we obtain $x_n - x_m - 2(n - m) < 0$, proving Eq. (S-26) because this inequality is contradicted with $x_j + 2 \leq x_{j+1}$.

II. DETERMINANTAL FORMULA FOR EQ. (5) IN THE MAIN TEXT

We shall prove that Eq. (5) in the main text can be expressed as a determinantal form. Using Eqs. (S-4) and (S-23), we can obtain

$$\Phi(x_1, \dots, x_N, t) = \sum_{\sigma \in \mathbb{S}_N} \int_{C_r} d\boldsymbol{\xi} \prod_{j=1}^N \xi_{\sigma_j}^{x_j - j - y_{\sigma_j} + \sigma_j - 1} e^{-iE_{\xi_j} t} \tag{S-29}$$

$$= \int_{C_r} d\boldsymbol{\xi} \det \left(\xi_k^{x_j - j - y_k + k - 1} e^{-iE_{\xi_j} t} \right)_{j, k \in \{1, \dots, N\}} \tag{S-30}$$

$$= \int_{C_r} d\boldsymbol{\xi} \det \left(\xi_k^{\tilde{x}_j - \tilde{y}_k - 1} e^{-iE_{\xi_j} t} \right)_{j, k \in \{1, \dots, N\}} \tag{S-31}$$

with the variables $\tilde{x}_j := x_j - j$ and $\tilde{y}_k := y_k - k$. Here, we use the definition of a determinant to derive the second line. When the initial state is the alternating domain-wall state ($y_j = 2j$), the exact many-body wavefunction becomes

$$\Phi(x_1, \dots, x_N, t) = \int d\xi \det \left(\xi_k^{x_j - j - k - 1} e^{-iE_{\xi_j} t} \right)_{j,k \in \{1, \dots, N\}}. \quad (\text{S-32})$$

We can explicitly show that the many-body wavefunction $\Phi(x_1, \dots, x_N, t)$ of Eq. (S-31) vanishes when there exists a site label j such that the relation $x_j + 1 = x_{j+1}$ holds. From Eq. (S-31), we obtain

$$\Phi(x_1, \dots, \underbrace{x_j}_j, \underbrace{x_{j+1}}_{j+1}, \dots, x_N, t) = \int_{C_r} d\xi \left(\prod_{k=1}^N e^{-iE_{\xi_k} t} \right) \det \left(\xi_l^{\tilde{x}_k - \tilde{y}_l - 1} \right)_{k,l \in \{1, \dots, N\}} \quad (\text{S-33})$$

$$= \int_{C_r} d\xi \left(\prod_{k=1}^N e^{-iE_{\xi_k} t} \right) \det \begin{pmatrix} \xi_1^{\tilde{x}_1 - \tilde{y}_1 - 1} & \dots & \xi_N^{\tilde{x}_1 - \tilde{y}_1 - 1} \\ \vdots & & \vdots \\ \xi_1^{\tilde{x}_j - \tilde{y}_1 - 1} & \dots & \xi_N^{\tilde{x}_j - \tilde{y}_1 - 1} \\ \xi_1^{\tilde{x}_j - \tilde{y}_1 - 1} & \dots & \xi_N^{\tilde{x}_j - \tilde{y}_1 - 1} \\ \vdots & & \vdots \\ \xi_1^{\tilde{x}_N - \tilde{y}_1 - 1} & \dots & \xi_N^{\tilde{x}_N - \tilde{y}_1 - 1} \end{pmatrix} \quad (\text{S-34})$$

$$= 0 \quad (\text{S-35})$$

To get the last line, we use the fact that the j and $(j+1)$ th rows of the matrix of Eq. (S-34) are identical.

III. PROOF OF EQ. (13) IN THE MAIN TEXT

We derive an exact many-body wavefunction $\Phi_{\text{XX}}(x_1, \dots, x_N, t)$ in the XX model, which is given in Eq. (13) in the main text. The Hamiltonian for the XX model is given as

$$\hat{H}_{\text{XX}} = \sum_{x \in \mathbb{Z}} (\hat{X}_x \hat{X}_{x+1} + \hat{Y}_x \hat{Y}_{x+1}). \quad (\text{S-36})$$

The initial state is

$$|\phi_{\text{XX}}(0)\rangle = \prod_{x=1}^N \hat{R}_{y_j} |0\rangle \quad (\text{S-37})$$

with $y_j + 1 \leq y_{j+1}$. Under this setup, the many-body wavefunction $\Phi_{\text{XX}}(x_1, \dots, x_N, t)$ obeys

$$i \frac{\partial}{\partial t} \Phi_{\text{XX}}(x_1, \dots, x_N, t) = \frac{1}{2} \sum_{j=1}^N \left(\Phi_{\text{XX}}(x_1, \dots, \underbrace{x_j + 1}_j, \dots, x_N, t) + \Phi_{\text{XX}}(x_1, \dots, \underbrace{x_j - 1}_j, \dots, x_N, t) \right) \quad (\text{S-38})$$

with the boundary condition defined by

$$\Phi_{\text{XX}}(x_1, \dots, \underbrace{x_j + 1}_j, \underbrace{x_{j+1}}_{j+1}, \dots, x_N, t) + \Phi_{\text{XX}}(x_1, \dots, \underbrace{x_j}_j, \underbrace{x_{j+1}}_{j+1}, \dots, x_N, t) = 0. \quad (\text{S-39})$$

The initial state of Eq. (S-37) reads

$$\Phi_{\text{XX}}(x_1, \dots, x_N, 0) = \prod_{j=1}^N \delta_{x_j, y_j}. \quad (\text{S-40})$$

Under this setup, the exact solutions for the many-body wavefunction becomes

$$\Phi_{\text{XX}}(x_1, \dots, x_N, t) = \int_{C_r} d\xi \sum_{\sigma \in \mathbb{S}_N} \text{sgn}(\sigma) \prod_{j=1}^N \xi_{\sigma_j}^{x_j - y_{\sigma_j} - 1} e^{-iE_{\xi_j} t}. \quad (\text{S-41})$$

In the following subsections, we prove that Eq. (S-41) solves Eqs. (S-38), (S-39), and (S-40).

A. Proof for Eq. (S-41) satisfying the equation (S-38) of motion

We substitute Eq. (S-41) into Eq. (S-38), obtaining

$$\text{LHS of Eq. (S-38)} = \int_{C_r} d\xi \sum_{\sigma \in \mathbb{S}_N} \text{sgn}(\sigma) \left(\sum_{k=1}^N E_{\xi_k} \right) \left(\prod_{j=1}^N \xi_{\sigma_j}^{x_j - y_{\sigma_j} - 1} e^{-iE_{\xi_j} t} \right), \quad (\text{S-42})$$

$$\text{RHS of Eq. (S-38)} = \frac{1}{2} \sum_{k=1}^N \int_{C_r} d\xi \sum_{\sigma \in \mathbb{S}_N} \text{sgn}(\sigma) (\xi_{\sigma_k} + \xi_{\sigma_k}^{-1}) \left(\prod_{j=1}^N \xi_{\sigma_j}^{x_j - y_{\sigma_j} - 1} e^{-iE_{\xi_j} t} \right) \quad (\text{S-43})$$

$$= \int_{C_r} d\xi \sum_{\sigma \in \mathbb{S}_N} \text{sgn}(\sigma) \left\{ \frac{1}{2} \sum_{k=1}^N (\xi_{\sigma_k} + \xi_{\sigma_k}^{-1}) \right\} \left(\prod_{j=1}^N \xi_{\sigma_j}^{x_j - y_{\sigma_j} - 1} e^{-iE_{\xi_j} t} \right) \quad (\text{S-44})$$

$$= \int_{C_r} d\xi \sum_{\sigma \in \mathbb{S}_N} \text{sgn}(\sigma) \left\{ \frac{1}{2} \sum_{k=1}^N (\xi_k + \xi_k^{-1}) \right\} \left(\prod_{j=1}^N \xi_{\sigma_j}^{x_j - y_{\sigma_j} - 1} e^{-iE_{\xi_j} t} \right) \quad (\text{S-45})$$

$$= \int_{C_r} d\xi \sum_{\sigma \in \mathbb{S}_N} \text{sgn}(\sigma) \left(\sum_{k=1}^N E_{\xi_k} \right) \left(\prod_{j=1}^N \xi_{\sigma_j}^{x_j - y_{\sigma_j} - 1} e^{-iE_{\xi_j} t} \right). \quad (\text{S-46})$$

Thus, we can prove that Eq. (S-41) satisfies the equation (S-38) of motion.

B. Proof for Eq. (S-41) satisfying the boundary condition of Eq. (S-39)

We substitute Eq. (S-41) into Eq. (S-39), obtaining

$$\text{LHS of Eq. (S-39)} \quad (\text{S-47})$$

$$= \int_{C_r} d\xi \sum_{\sigma \in \mathbb{S}_N} \text{sgn}(\sigma) \left(\prod_{l \in \{1, \dots, N\}; l \neq j, j+1} \xi_{\sigma_l}^{x_l - y_{\sigma_l} - 1} e^{-iE_{\xi_l} t} \right) e^{-i(E_{\xi_j} + E_{\xi_{j+1}})t} \left(\xi_{\sigma_j}^{x_j - y_{\sigma_j}} \xi_{\sigma_{j+1}}^{x_{j+1} - y_{\sigma_{j+1}}} + \xi_{\sigma_j}^{x_j - y_{\sigma_j} - 1} \xi_{\sigma_{j+1}}^{x_{j+1} - y_{\sigma_{j+1}} - 1} \right) \quad (\text{S-48})$$

$$= \int_{C_r} d\xi \sum_{\sigma \in \mathbb{S}_N} \text{sgn}(\sigma) \left(\prod_{l \in \{1, \dots, N\}; l \neq j, j+1} \xi_{\sigma_l}^{x_l - y_{\sigma_l} - 1} e^{-iE_{\xi_l} t} \right) e^{-i(E_{\xi_j} + E_{\xi_{j+1}})t} \xi_{\sigma_j}^{x_j - y_{\sigma_j}} \xi_{\sigma_{j+1}}^{x_{j+1} - y_{\sigma_{j+1}}} (1 + \xi_{\sigma_j}^{-1} \xi_{\sigma_{j+1}}^{-1}) \quad (\text{S-49})$$

$$= \int_{C_r} d\xi \sum_{\sigma \in \mathbb{S}_N} G_{\sigma}^{\text{XX}}(\xi, j). \quad (\text{S-50})$$

Here, we define the function $G_{\sigma}^{\text{XX}}(\xi, j)$ as

$$G_{\sigma}^{\text{XX}}(\xi, j) := \text{sgn}(\sigma) \left(\prod_{l \in \{1, \dots, N\}; l \neq j, j+1} \xi_{\sigma_l}^{x_l - y_{\sigma_l} - 1} e^{-iE_{\xi_l} t} \right) e^{-i(E_{\xi_j} + E_{\xi_{j+1}})t} \xi_{\sigma_j}^{x_j - y_{\sigma_j}} \xi_{\sigma_{j+1}}^{x_{j+1} - y_{\sigma_{j+1}}} (1 + \xi_{\sigma_j}^{-1} \xi_{\sigma_{j+1}}^{-1}). \quad (\text{S-51})$$

Using the permutation μ defined in Eq. (S-15) for a fixed permutation σ , we can prove

$$G_{\sigma}^{\text{XX}}(\xi, j) + G_{\mu}^{\text{XX}}(\xi, j) \quad (\text{S-52})$$

$$= \text{sgn}(\sigma) \left(\prod_{l \in \{1, \dots, N\}; l \neq j, j+1} \xi_{\sigma_l}^{x_l - y_{\sigma_l} - 1} e^{-iE_{\xi_l} t} \right) e^{-i(E_{\xi_j} + E_{\xi_{j+1}})t} \xi_{\sigma_j}^{x_j - y_{\sigma_j}} \xi_{\sigma_{j+1}}^{x_{j+1} - y_{\sigma_{j+1}}} \{1 + \xi_{\sigma_j}^{-1} \xi_{\sigma_{j+1}}^{-1} - (1 + \xi_{\sigma_{j+1}}^{-1} \xi_{\sigma_j}^{-1})\} \quad (\text{S-53})$$

$$= 0. \quad (\text{S-54})$$

This completes the proof.

C. Proof for Eq. (S-41) satisfying the initial state of Eq. (S-40)

We give a detailed proof for $\Phi_{XX}(x_1, \dots, x_N, 0) = \prod_{j=1}^N \delta_{x_j, y_j}$ using Eq. (S-41). Let me put $t = 0$ into Eq. (S-41):

$$\Phi_{XX}(x_1, \dots, x_N, 0) = \sum_{\sigma \in \mathbb{S}_N} \text{sgn}(\sigma) \prod_{j=1}^N \delta_{x_j, y_{\sigma_j}} \quad (\text{S-55})$$

$$= \prod_{j=1}^N \delta_{x_j, y_j}. \quad (\text{S-56})$$

The equality of Eq. (S-56) is proved by considering the inequalities $x_j + 1 \leq x_{j+1}$ and $y_j + 1 \leq y_{j+1}$. Suppose that there is an inversion in a given σ such that $\sigma_m > \sigma_n$ holds for $m < n$. From the inequalities $x_j + 1 \leq x_{j+1}$ and $y_j + 1 \leq y_{j+1}$, elementary calculation leads to $x_n - x_m \geq n - m$ and $y_{\sigma_m} - y_{\sigma_n} \geq \sigma_m - \sigma_n$. Then we can show an inequality $x_n - x_m + m - n < 0$ by

$$x_n - x_m + m - n = y_{\sigma_n} - y_{\sigma_m} + m - n \quad (\text{S-57})$$

$$\leq \underbrace{\sigma_n - \sigma_m}_{<0} + \underbrace{m - n}_{<0} \quad (\text{S-58})$$

This proves the equality of Eq. (S-56).

D. Determinantal formula for the exact many-body wavefunction

We derive the determinantal formulation for the many-body wavefunction. Using Eq. (S-41) and the definition of a determinant, we obtain

$$\Phi_{XX}(x_1, \dots, x_N, t) = \int_{C_r} d\xi \det \left(\xi_k^{x_j - y_k - 1} e^{-iE_{\xi_j} t} \right)_{j, k \in \{1, \dots, N\}}. \quad (\text{S-59})$$

When the initial state is the domain-wall state ($y_j = j$), we obtain

$$\Phi_{XX}(x_1, \dots, x_N, t) = \int_{C_r} d\xi \det \left(\xi_k^{x_j - k - 1} e^{-iE_{\xi_j} t} \right)_{j, k \in \{1, \dots, N\}}. \quad (\text{S-60})$$

This completes the poof of Eq. (13).

IV. ASYMPTOTIC ANALYSIS TO THE GUE TRACY-WIDOM DISTRIBUTION WITH FAST CONVERGENCE

In the main text, we derive the GUE Tracy-Widom distribution using the scaling variable s defined through $x = 2 + \lfloor -t - (t/2)^{1/3}s \rfloor$. This definition of the scaling variable s is based on the previous work [32]. In this section, we introduce another scaling variable u defined through $x = 2 + \lfloor -t - a - (t/2)^{1/3}u \rfloor$ with the fixed parameter a , explaining that the choice of the value $a = 1/2$ leads to faster convergence of $F(x, t)$ to the GUE Tracy-Widom distribution in comparison with the previous work with $a = 0$. This fast convergence was mathematically studied in the context of classical stochastic processes in Ref. [61], which investigated finite-time corrections to nonequilibrium fluctuations in classical models belonging to the Kardar-Parisi-Zhang universality class. We here explain this result with language familiar with physicists. If readers prefer the mathematically rigorous treatment, we recommend them to check the proposition 3.2 of Ref. [61].

A. Explanation for the asymptotic analysis with fast convergence

First, following the calculation of Ref. [32], we rewrite the kernel $K_B(t, m, n)$ in the main text by using the formula $J_{m-1}(t) = J'_m(t) + \frac{m}{t}J_m(t)$:

$$K_B(t, m, n) = \sum_{l=-\infty}^{-1} J_{m-l}(t) J_{n-l}(t) \quad (\text{S-61})$$

$$= \frac{t}{2(m-n)} (J'_m(t) J_n(t) - J_m(t) J'_n(t)) - \frac{1}{2} J_m(t) J_n(t). \quad (\text{S-62})$$

Here, $J'_m(t)$ is the Bessel function of the first kind differentiated with respect to t .

Second, we revisit the asymptotic analysis for the Bessel function of the first kind. We employ the asymptotic analysis for $t \gg 1$, obtaining

$$J_{\lfloor t+a+(t/2)^{1/3}u \rfloor}(t) \simeq \left(\frac{2}{t}\right)^{1/3} \text{Ai}\left(u + a\left(\frac{2}{t}\right)^{1/3}\right), \quad (\text{S-63})$$

$$J'_{\lfloor t+a+(t/2)^{1/3}u \rfloor}(t) \simeq -\left(\frac{2}{t}\right)^{2/3} \text{Ai}'\left(u + a\left(\frac{2}{t}\right)^{1/3}\right), \quad (\text{S-64})$$

where $\text{Ai}'(x)$ denote the Airy function differentiated with respect to x . The derivations of these asymptotic formulae are described in the subsequent subsections.

Third, we introduce continuous variables v and w through $m = \lfloor t + a + (t/2)^{1/3}v \rfloor$ and $n = \lfloor t + a + (t/2)^{1/3}w \rfloor$, substituting Eqs. (S-63) and (S-64) into Eq. (S-68). As a result, we obtain

$$\begin{aligned} & K_B(t, \lfloor t + a + (t/2)^{1/3}v \rfloor, \lfloor t + a + (t/2)^{1/3}w \rfloor) \\ & \simeq \left(\frac{2}{t}\right)^{1/3} \frac{1}{v-w} \left[\text{Ai}'\left(v + a\left(\frac{2}{t}\right)^{1/3}\right) \text{Ai}\left(w + a\left(\frac{2}{t}\right)^{1/3}\right) - \text{Ai}\left(v + a\left(\frac{2}{t}\right)^{1/3}\right) \text{Ai}'\left(w + a\left(\frac{2}{t}\right)^{1/3}\right) \right] \\ & \quad - \frac{1}{2} \left(\frac{2}{t}\right)^{2/3} \text{Ai}\left(v + a\left(\frac{2}{t}\right)^{1/3}\right) \text{Ai}\left(w + a\left(\frac{2}{t}\right)^{1/3}\right). \end{aligned} \quad (\text{S-65})$$

Finally, we expand the Airy function in Eq. (S-70) with respect to the small quantity $a(2/t)^{1/3}$. Using the differential equation for the Airy function, namely $d^2\text{Ai}(x)/dx^2 = x\text{Ai}(x)$, we get

$$K_B(t, m, n) \simeq \left(\frac{2}{t}\right)^{1/3} K_{\text{Ai}}(v, w) + \left(a - \frac{1}{2}\right) \left(\frac{2}{t}\right)^{2/3} \text{Ai}(v) \text{Ai}(w). \quad (\text{S-66})$$

Here, we define the Airy kernel $K_{\text{Ai}}(v, w)$ by

$$K_{\text{Ai}}(v, w) := \frac{\text{Ai}(v) \text{Ai}'(w) - \text{Ai}'(v) \text{Ai}(w)}{v-w}. \quad (\text{S-67})$$

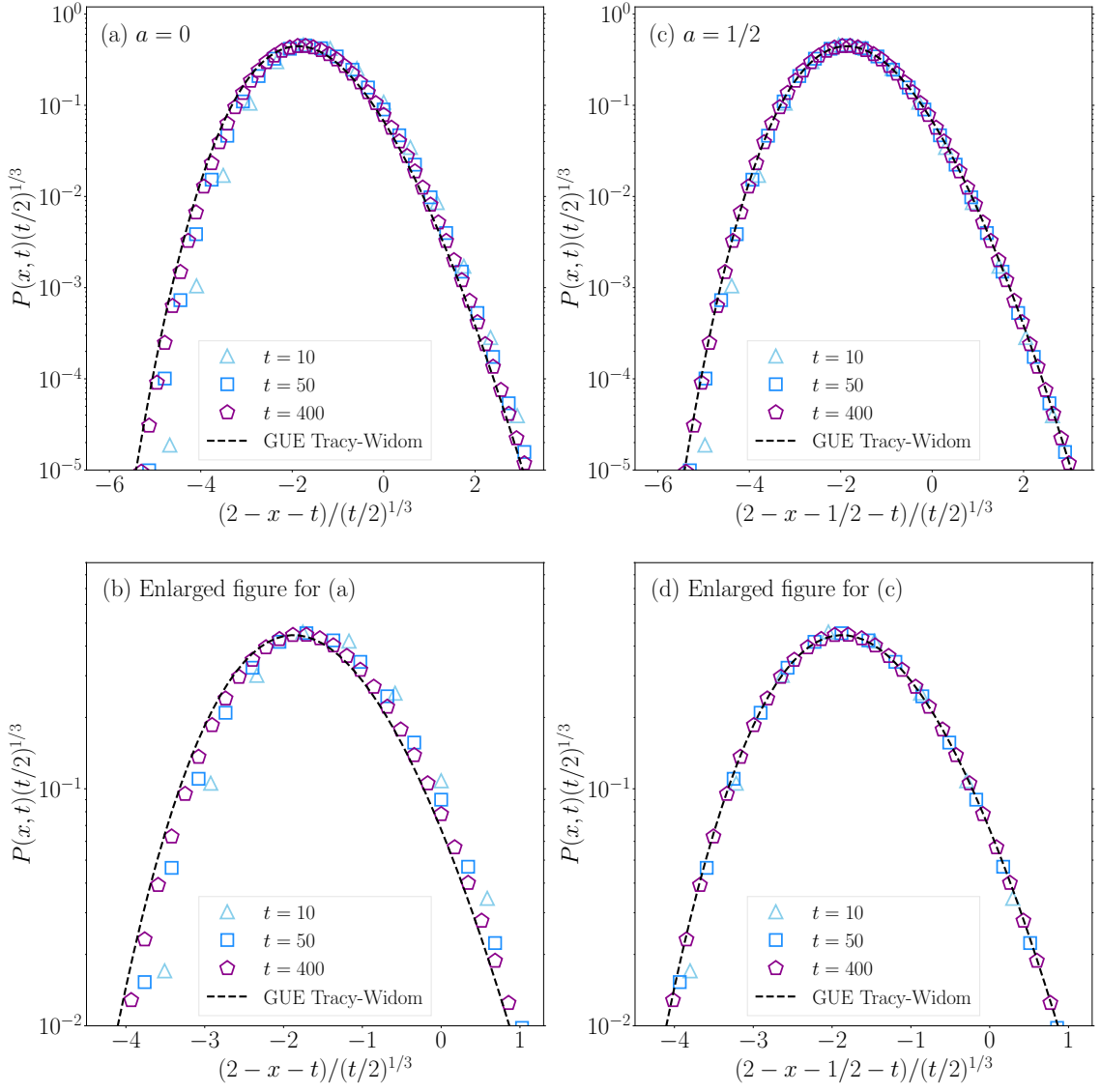


FIG. S-1. Numerical test for the fast convergence of $P(x,t)$ to the probability density function for the GUE Tracy-Widom distribution. The probability $P(x,t)$ is numerically computed using Eq. (S-68). We show the data with $a = 0$ [$a = 1/2$] in (a) [(c)], and the corresponding enlarged figure is shown in (b) [(d)]. The dashed lines represent the probability density function $dF_2(s)/ds$ for the GUE Tracy-Widom distribution.

The previous works [32, 33] set $a = 0$, and thus the last term of Eq. (S-66), which is proportional to $(2/t)^{2/3}$, survives in the *finite time regions*. However, when setting $a = 1/2$, the term vanishes. As a result, we can expect that the kernel $K_B(t, m, n)$ converges to the Airy kernel $K_{Ai}(v, w)$ faster.

B. Numerical test for the fast convergence

We numerically test the fact that the choice of $a = 1/2$ leads to the fast convergence of $F(x,t)$ to the GUE Tracy-Widom distribution. The formula used here is Eq. (10) of the main text, which is given by

$$F(x,t) = \det(1 - K_B(t, m, n))_{l^2(\{2-x, 3-x, \dots\})} \quad (\text{S-68})$$

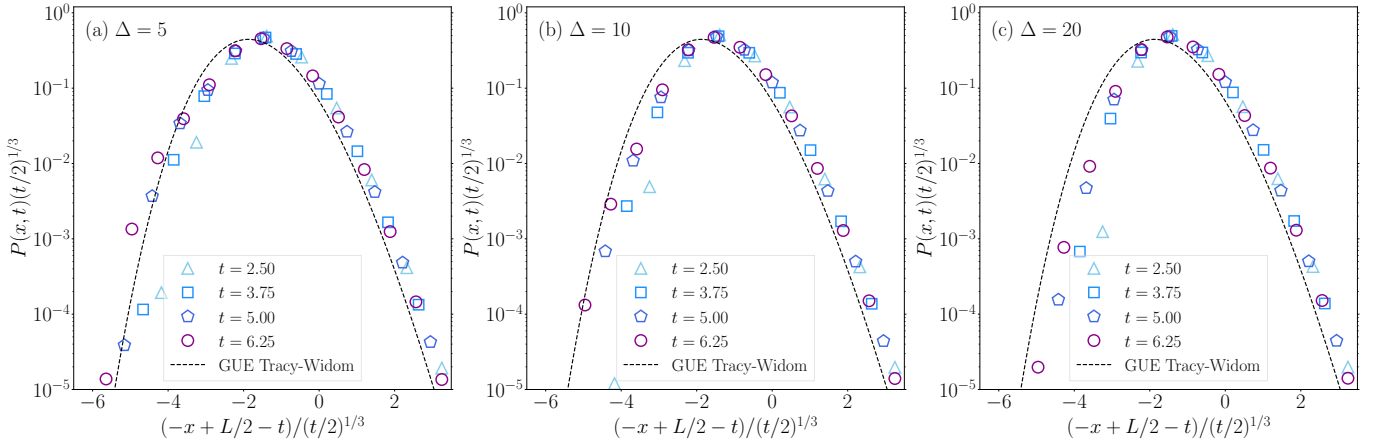


FIG. S-2. Time evolution for the probability $P(x, t)$ in the XXZ model with $\Delta =$ (a) 5, (b) 10, and (c) 20. The numerical data displayed in these figures are sama as those in Fig. 2 of the main text. A point being different from Fig. 2 of the main text is the abscissa. We here use the scale with $a = 0$ while do the one with $a = 1/2$ in Fig. 2 of the main text. The dashed lines represent the probability density function $dF_2(s)/ds$ for the GUE Tracy-Widom distribution.

with

$$K_B(t, m, n) = \frac{t J_m(t) J_{n+1}(t) - J_{m+1}(t) J_n(t)}{2(m-n)} \quad (\text{S-69})$$

$$= \sum_{l=-\infty}^{-1} J_{m-l}(t) J_{n-l}(t). \quad (\text{S-70})$$

Note that Eq. (S-70) is used when calculating the diagonal element $K_B(t, m, m)$. Using them, we can numerically obtain the probability $P(x, t) = F(x, t) - F(x + 1, t)$ of finding the left-most up-spin at site x and time t . In the case of Eq. (S-68), we use the scaling variable u defined through $2 - x = \lfloor t + a + (t/2)^{1/3} u \rfloor$, expecting that the choice of $a = 1/2$ will exhibit faster convergence of $F(x, t)$ to the GUE Tray-Widom distribution in comparison with the case with $a = 0$.

Figure S-1 showcases the numerical results for the time evolution of $P(x, t)$ computed by Eq. (S-68). In Figs. S-1(a) and (b), we plot the numerical data with $a = 0$ for the rescaled abscissa and ordinate, while the numerical data with $a = 1/2$ are shown in Figs. S-1(c) and (d). All the results exhibit that the deviations from the GUE Tracy-Widom decrease in time, but one can clearly see speed of the convergence to the GUE Tracy-Widom in the case with $a = 1/2$ is faster than that with $a = 0$.

In Fig. 2 of main text, we use $a = 1/2$, finding the good agreement with the GUE Tracy-Widom distribution. For comparison with Fig. 2 of main text, we also display the same data with $a = 0$ in Fig. S-2, where the deviations from the GUE Tracy-Widom are large.

C. Derivation of Eq. (S-63)

We shall derive Eq. (S-63) using the asymptotic analysis. The integral representation for $J_n(t)$ is given by

$$J_n(t) = \frac{1}{2\pi e^{i\pi n/2}} \int_0^{2\pi} d\theta \exp(in\theta + it \cos \theta). \quad (\text{S-71})$$

Putting $n = \lfloor t + a + (t/2)^{1/3} u \rfloor$ into the above for $t \gg 1$, we derive

$$J_{\lfloor t + a + (t/2)^{1/3} u \rfloor}(t) \simeq \frac{1}{2\pi e^{i\pi(t + a + (t/2)^{1/3} u)/2}} \int_0^{2\pi} d\theta \exp \left\{ i \left[a + \left(\frac{t}{2} \right)^{1/3} u \right] \theta + it(\theta + \cos \theta) \right\} \quad (\text{S-72})$$

$$\simeq \frac{1}{2\pi e^{i\pi(t + a + (t/2)^{1/3} u)/2}} \int_0^{2\pi} d\theta \exp \left\{ i \left[a + \left(\frac{t}{2} \right)^{1/3} u \right] \theta + it \left[\frac{\pi}{2} + \frac{1}{6} \left(\theta - \frac{\pi}{2} \right)^3 \right] \right\} \quad (\text{S-73})$$

$$= \frac{1}{2\pi} \int_{-\pi/2}^{3\pi/2} d\phi \exp \left\{ i \left[a + \left(\frac{t}{2} \right)^{1/3} u \right] \phi + i \frac{t}{6} \phi^3 \right\} \quad (\text{S-74})$$

$$\simeq \frac{1}{2\pi} \left(\frac{2}{t} \right)^{1/3} \int_{-\infty}^{\infty} d\psi \exp \left\{ i \left[u + a \left(\frac{2}{t} \right)^{1/3} \right] \psi + i \frac{\psi^3}{3} \right\} \quad (\text{S-75})$$

$$= \left(\frac{2}{t} \right)^{1/3} \text{Ai} \left(u + a \left(\frac{2}{t} \right)^{1/3} \right). \quad (\text{S-76})$$

In Eq. (S-73), we expand the function $\theta + \cos \theta$ around $\pi/2$ since $e^{it(\theta + \cos \theta)}$ rapidly oscillate as a function of θ for $t \gg 1$. To derive the last equality, we use the integral formula given by

$$\text{Ai}(x) = \frac{1}{\pi} \int_0^{\infty} d\theta \cos \left(x\theta + \frac{\theta^3}{3} \right). \quad (\text{S-77})$$

This completes the derivation of Eq. (S-63).

D. Derivation of Eq. (S-64)

We shall derive Eq. (S-64) using the asymptotic analysis. Following the calculation being similar to the above, we have

$$J'_{[t+a+(t/2)^{1/3}u]}(t) \simeq \frac{1}{2\pi e^{i\pi(t+a+(t/2)^{1/3}u)/2}} \int_0^{2\pi} d\theta \cos \theta \exp \left\{ i \left[a + \left(\frac{t}{2} \right)^{1/3} u \right] \theta + it(\theta + \cos \theta) \right\} \quad (\text{S-78})$$

$$\simeq \frac{1}{2\pi e^{i\pi(t+a+(t/2)^{1/3}u)/2}} \int_0^{2\pi} d\theta \cos \theta \exp \left\{ i \left[a + \left(\frac{t}{2} \right)^{1/3} u \right] \theta + it \left[\frac{\pi}{2} + \frac{1}{6} \left(\theta - \frac{\pi}{2} \right)^3 \right] \right\} \quad (\text{S-79})$$

$$= \frac{1}{2\pi} \int_{-\pi/2}^{3\pi/2} d\phi \cos(\pi/2 + \phi) \exp \left\{ i \left[a + \left(\frac{t}{2} \right)^{1/3} u \right] \phi + i \frac{t}{6} \phi^3 \right\} \quad (\text{S-80})$$

$$\simeq -\frac{1}{2\pi} \left(\frac{2}{t} \right)^{2/3} \int_{-\infty}^{\infty} d\psi \psi \exp \left\{ i \left[u + a \left(\frac{2}{t} \right)^{1/3} \right] \psi + i \frac{\psi^3}{3} \right\} \quad (\text{S-81})$$

$$= -\left(\frac{2}{t} \right)^{2/3} \text{Ai}' \left(u + a \left(\frac{2}{t} \right)^{1/3} \right). \quad (\text{S-82})$$

Here, we use the integral formula given by

$$\text{Ai}'(x) = -\frac{1}{\pi} \int_0^{\infty} d\theta \theta \sin \left(x\theta + \frac{\theta^3}{3} \right). \quad (\text{S-83})$$

This completes the derivation of Eq. (S-64).

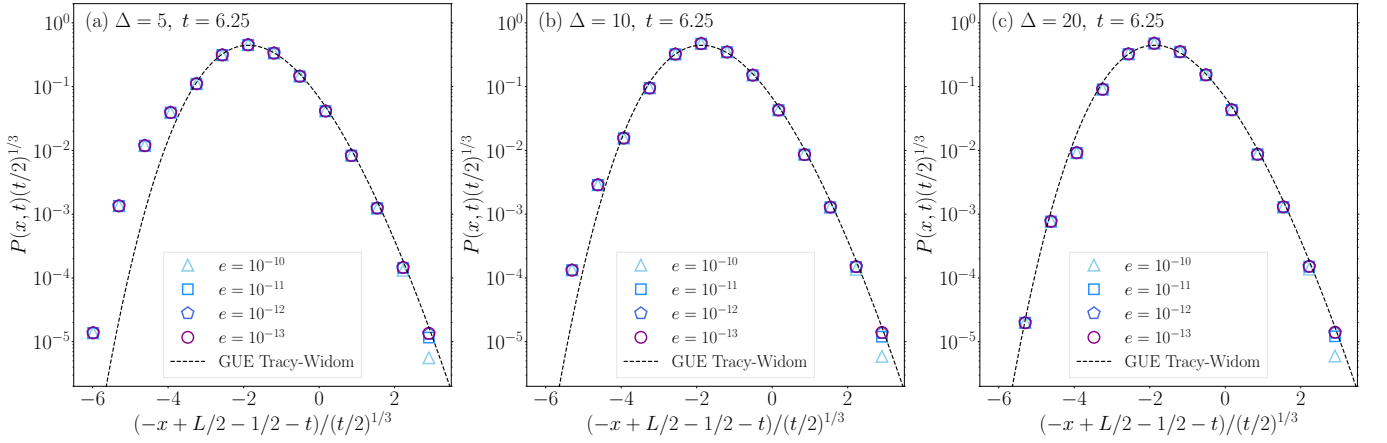


FIG. S-3. Probability $P(x, t)$ at $t = 6.25$ in the XXZ model with $\Delta =$ (a) 5, (b) 10, and (c) 20. In each panel, the probabilities $P(x, t)$ with the threshold parameter $e = 10^{-10}, 10^{-11}, 10^{-12}$ and 10^{-13} are shown. The numerical data with $e = 10^{-13}$ displayed in these figures are sama as those in Fig. 2 of the main text. The dashed lines represent the probability density function $dF_2(s)/ds$ for the GUE Tracy-Widom distribution.

V. NUMERICAL TRUNCATION IN THE TEBD METHOD

We show numerical evidences that our numerical results for the probability $P(x, t)$ well converge in the framework of the TEBD method [47–50]. In this numerical method, we expand a quantum state $|\psi\rangle$ by the Vidal’s canonical form given by

$$|\psi\rangle = \sum_{\sigma_1=1}^2 \cdots \sum_{\sigma_L=1}^2 \psi(\sigma_1, \dots, \sigma_L) |\sigma_1, \dots, \sigma_L\rangle, \quad (\text{S-84})$$

$$\psi(\sigma_1, \dots, \sigma_L) = \sum_{\sigma_1=1}^2 \sum_{\alpha_1=1}^{\chi_1} \cdots \sum_{\sigma_{N-1}=1}^2 \sum_{\alpha_{N-1}=1}^{\chi_{N-1}} \sum_{\sigma_N=1}^2 \Gamma_{\alpha_1}^{[1], \sigma_1} \lambda_{\alpha_1}^{[1]} \Gamma_{\alpha_1, \alpha_2}^{[2], \sigma_2} \lambda_{\alpha_2}^{[2]} \dots \Gamma_{\alpha_{N-2}, \alpha_{N-1}}^{[N-1], \sigma_{N-1}} \lambda_{\alpha_{N-1}}^{[N-1]} \Gamma_{\alpha_{N-1}}^{[N], \sigma_N}. \quad (\text{S-85})$$

Here, λ and Γ , indices of which are abbreviated, are real and complex coefficients for the many-body wavefunction $\psi(\sigma_1, \dots, \sigma_L)$, respectively, and χ_j represents a bond dimension between site j and site $j + 1$. In general, the bond dimension χ_j depends on time t during dynamics, and we have

$$\sum_{\alpha=1}^{\chi_j} (\lambda_{\alpha}^{[j]})^2 = 1 \quad (\text{S-86})$$

if we do not truncate the bond dimension. In what follows, we assume that $\lambda_{\alpha}^{[j]}$ is in decreasing order in the label α . In numerical calculations based on the TEBD method, one usually truncates the bond dimension. To be more specific, we set a threshold parameter $e \in \mathbb{R}$ and discard small $\lambda_{\alpha}^{[j]}$ such that the following inequality holds:

$$\left| \sum_{\alpha=1}^{\chi_j^{\text{trun}}} (\lambda_{\alpha}^{[j]})^2 - 1 \right| < e, \quad (\text{S-87})$$

where χ_j^{trun} indicates the truncated bond dimension. In this numerical method, we need to confirm that the numerical data converges by systematically changing a value of e for the truncation of the bond dimension.

Figure S-3 showcases numerical data for $P(x, t)$ at $t = 6.25$ obtained by changing a value of the threshold parameter e . We find that the numerical data of $P(x, t)$ with $e = 10^{-13}$, which is displayed in Fig. 2 of the main text, are well convergent.

VI. LIMITING PROBABILITY DISTRIBUTION FUNCTION FOR $\Delta = 0$

We shall derive the limiting probability distribution function for the left-most up-spin in the dynamics of the XXZ model with $\Delta = 0$. The initial state is the alternating domain-wall state $|\phi(0)\rangle = \prod_{x=1}^{\infty} \hat{R}_{2x} |0\rangle$. Our following derivation here is based on Ref. [32] of the main text.

First, we analytically derive a probability distribution function $F_{\text{XX}}(x, t)$ of finding the left-most up-spin at site x and time t . For this purpose, we introduce a generating function $G(x, t, \lambda)$ as

$$G(x, t, \lambda) := \langle \phi(t) | e^{-\lambda \hat{N}_x} | \phi(t) \rangle \quad (\text{S-88})$$

with $\hat{N}_x := \sum_{j=-\infty}^x (\hat{Z}_j + 1/2)$. Since the XXZ model with $\Delta = 0$ can be mapped into a Hamiltonian for noninteracting fermions via the Jordan-Wigner transformation, we can get

$$G(x, t, \lambda) = \det \left[1 + (e^{-\lambda} - 1) K_{\text{XX}}(t, m, n) \right]_{l^2(\{-x, -x+1, \dots\})}, \quad (\text{S-89})$$

where the function $K_{\text{XX}}(t, m, n)$ is defined by

$$K_{\text{XX}}(t, m, n) := \sum_{k=1}^{\infty} J_{m+2k}(t) J_{n+2k}(t) \quad (\text{S-90})$$

Taking the large λ limit, we obtain the probability $P_0(x, t)$ for finding no up-spins in the region $\{x, x-1, \dots\}$:

$$P_0(x, t) = \det \left[1 - K_{\text{XX}}(t, m, n) \right]_{l^2(\{-x, -x+1, \dots\})}. \quad (\text{S-91})$$

This result leads to

$$F_{\text{XX}}(x, t) = P_0(x-1, t) = \det \left(1 - K_{\text{XX}}(t, m, n) \right)_{l^2(\{-x+1, -x+2, \dots\})}. \quad (\text{S-92})$$

Second, we shall take the long-time limit for $K_{\text{XX}}(t, m, n)$ using scaling variables y and z defined through $m = 1 - \lfloor t + (t/2)^{1/3} y \rfloor$ and $n = 1 - \lfloor t + (t/2)^{1/3} z \rfloor$. Following the conventional asymptotic analysis described in Sec. IV, we obtain

$$K_{\text{XX}}(t, 1 - \lfloor t + (t/2)^{1/3} y \rfloor, 1 - \lfloor t + (t/2)^{1/3} z \rfloor) \simeq \left(\frac{2}{t} \right)^{2/3} \sum_{k=1}^{\infty} \text{Ai} \left(y + 2k \left(\frac{2}{t} \right)^{1/3} \right) \text{Ai} \left(z + 2k \left(\frac{2}{t} \right)^{1/3} \right) \quad (t \gg 1). \quad (\text{S-93})$$

Next we introduce a new variable $w_k := 2k \left(\frac{2}{t} \right)^{1/3}$, for which the unit of this discretized variable is given by $2 \left(\frac{2}{t} \right)^{1/3}$. As a result, we eventually get

$$K_{\text{XX}}(t, 1 - \lfloor t + (t/2)^{1/3} y \rfloor, 1 - \lfloor t + (t/2)^{1/3} z \rfloor) \simeq \frac{1}{2} \left(\frac{2}{t} \right)^{1/3} \int_0^{\infty} dw \text{Ai}(y+w) \text{Ai}(z+w) \quad (t \gg 1). \quad (\text{S-94})$$

Third, we take the long-time limit for $F_{\text{XX}}(x, t)$ itself by employing Eq. (S-94) and a scaling variable s defined through $x = 1 - \lfloor t + (t/2)^{1/3} s \rfloor$. We apply the Fredholm expansion to Eq. (S-92), obtaining for $t \gg 1$,

$$F_{\text{XX}}(1 - \lfloor t + (t/2)^{1/3} s \rfloor, t) = 1 + \sum_{k=1}^{\infty} \frac{(-1)^k}{k!} \sum_{l_1=-x+1}^{\infty} \cdots \sum_{l_k=-x+1}^{\infty} \det [K_{\text{XX}}(t, m, n)]_{m, n \in \{l_1, \dots, l_k\}} \quad (\text{S-95})$$

$$\simeq 1 + \sum_{k=1}^{\infty} \frac{(-1)^k}{k!} \sum_{l_1=-x+1}^{\infty} \cdots \sum_{l_k=-x+1}^{\infty} \left(\frac{2}{t} \right)^{k/3} \det \left[\frac{1}{2} \int_0^{\infty} dw \text{Ai}(y_m + w) \text{Ai}(y_n + w) \right]_{m, n \in \{1, \dots, k\}} \quad (\text{S-96})$$

$$\simeq 1 + \sum_{k=1}^{\infty} \frac{(-1)^k}{k!} \int_s^{\infty} dy_1 \cdots \int_s^{\infty} dy_k \det \left[\frac{1}{2} \int_0^{\infty} dw \text{Ai}(y_m + w) \text{Ai}(y_n + w) \right]_{m, n \in \{1, \dots, k\}} \quad (\text{S-97})$$

$$= \text{Det} \left[1 - \frac{1}{2} K_{\text{Ai}}(x, y) \right]_{\mathbb{L}^2(s, \infty)} \quad (\text{S-98})$$

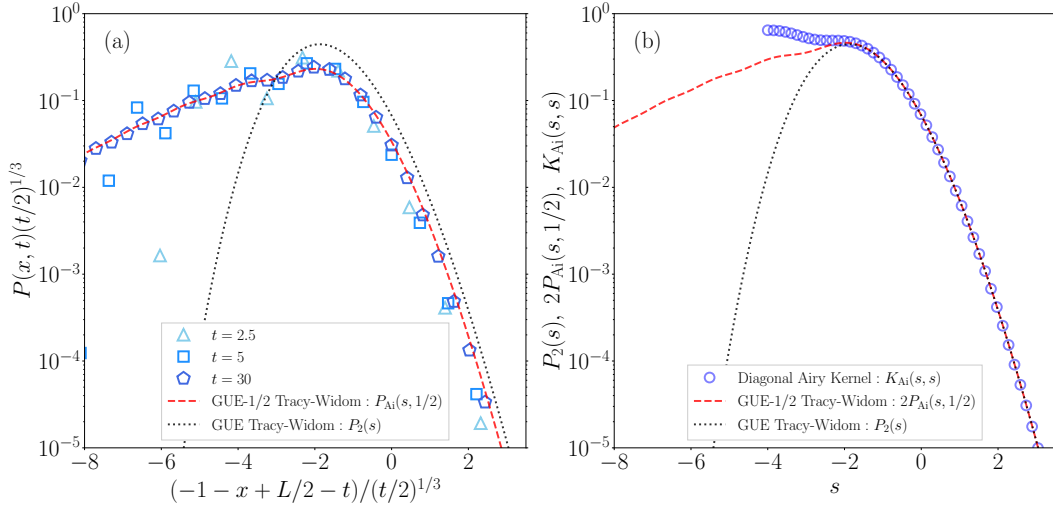


FIG. S-4. (a) Probability density functions $P_2(s)$ and $P_{\text{Ai}}(s, 1/2)$, and a rescaled probability $P(x, t)$ for the XXZ model with $\Delta = 0$. The functions $P_2(s)$ and $P_{\text{Ai}}(s, 1/2)$ denote the probability density function for the GUE Tracy-Widom distribution $F_2(s)$ and $F_{\text{Ai}}(s, 1/2)$ of Eq. (S-99). The numerical setup for the XXZ model with $\Delta = 0$ is same as Fig. 2 of the main text. (b) Comparison for $P_2(s)$, $2P_{\text{Ai}}(s, 1/2)$, and $K_{\text{Ai}}(s, s)$.

$$= F_{\text{Ai}}(s, 1/2). \quad (\text{S-99})$$

Here, we use the variable y_m through $l_m = 1 - [t + (t/2)^{1/3}y_m]$ in the second line, the Airy Kernel $K_{\text{Ai}}(x, y) = (\text{Ai}(x)\text{Ai}'(y) - \text{Ai}'(x)\text{Ai}(y))/(x - y)$ in the fourth line, and $F_{\text{Ai}}(s, a) := \text{Det}[1 - aK_{\text{Ai}}(x, y)]_{\mathbb{L}^2(s, \infty)}$ in the fifth line. The expression of $F_{\text{Ai}}(s, 1/2)$ is different from the GUE Tracy-Widom distribution function $F_2(s) = \text{Det}[1 - K_{\text{Ai}}(x, y)]_{\mathbb{L}^2(s, \infty)}$ by the factor $1/2$ in front of the Airy Kernel.

Figure S-4 (a) displays the probability density functions $P_2(s) := dF_2(s)/ds$ and $P_{\text{Ai}}(s, 1/2) = dF_{\text{Ai}}(s, 1/2)/ds$, and the time dependent probability $P(x, t)$ in the XXZ model with $\Delta = 0$. The probability density functions $P_2(s)$ and $P_{\text{Ai}}(s, 1/2)$ are numerically computed via the Bornemann method [89] and the probability $P(x, t)$ for the XXZ model with $\Delta = 0$ is numerically calculated under the same setup of Fig. 2 of the main text. We find that the function $P_{\text{Ai}}(s, 1/2)$ shows large deviations from $P_2(s)$ especially in the left region and the probability $P(x, t)$ becomes closer to $P_{\text{Ai}}(s, 1/2)$ as time goes by. In Fig. S-4 (b), we show $P_2(s)$, $2P_{\text{Ai}}(s, 1/2)$, and $K_{\text{Ai}}(s, s)$, finding that they are almost same in the right region. This can be understood by noting that the Airy function is small in the right region. Taking this fact into account, we obtain the approximated expressions in the right region, which are given by

$$P_2(s) \simeq K_{\text{Ai}}(s, s), \quad (\text{S-100})$$

$$P_{\text{Ai}}(s, 1/2) \simeq \frac{1}{2}K_{\text{Ai}}(s, s). \quad (\text{S-101})$$

This demonstrates the behavior of Fig. S-4(b).

Finally, we consider the dynamics of the XXZ model with $\Delta = 0$ starting from the generalized domain-wall state $|\phi(0)\rangle = \prod_{x=1}^{\infty} \hat{R}_{\alpha x} |0\rangle$ characterized by a positive integer α . Following almost the same calculations explained just above, we can derive

$$F_{\text{XX}}(1 - [t + (t/2)^{1/3}s], t) \simeq F_{\text{Ai}}(s, 1/\alpha) \quad (t \gg 1). \quad (\text{S-102})$$

Then, the corresponding probability $P(x, t)$ with $x = 1 - [t + (t/2)^{1/3}s]$ in the right region is approximately given by

$$P_{\text{Ai}}(s, 1/\alpha) \simeq \frac{1}{\alpha}K_{\text{Ai}}(s, s). \quad (\text{S-103})$$

Therefore, the curve of $P(x, t)$ characterized by the diagonal Airy Kernel is universal in the sense that it appears irrespective of α .

VII. CONJECTURE FOR THE XXZ MODEL BY SAENZ, TRACY, AND WIDOM

We explain our discussion concerning the universal behavior in the XXZ model, which is described in the main text, after introducing the conjecture given by Saenz, Tracy, and Widom in Ref. [33].

We first describe the conjecture. The Hamiltonian \hat{H} used in Ref. [33] is

$$\hat{H} = 2 \sum_{x \in \mathbb{Z}} (\hat{X}_{x+1} \hat{X}_x + \hat{Y}_{x+1} \hat{Y}_x + \Delta \hat{Z}_{x+1} \hat{Z}_x). \quad (\text{S-104})$$

The initial state is $\prod_{j=1}^N \hat{R}_{y_j} |0\rangle$ with the integer y_j ($j \in \{1, 2, \dots, N\}$). The quantity of the interest is a probability $\mathcal{F}_N(x, t)$ for finding the left-most up-spin smaller than x at time t . Under this setup, Saenz, Tracy, and Widom proposed the following conjecture:

Conjecture (Ref. [33] of the main text). *As $t \gg N \rightarrow \infty$, $\mathcal{F}_N(x, t)$, with $x = -2t - st^{-1/3}$ and $y_j + 1 = v_j t^{-1/3}$, equals to the limit of*

$$\sum_{\sigma \in \mathbb{S}_N} (-1)^\sigma \sum_{S \subset [N]} (-1)^{|S|} t^{-|S|/3} F(\sigma, S) \prod_{k \in S} \mathbf{K}_{\text{Ai}}(s + v_{\sigma(k)}, s + v_k) \quad (\text{S-105})$$

with the set $[N] = \{1, 2, \dots, N\}$. The functions $\mathbf{K}_{\text{Ai}}(x, y)$ and $F(\sigma, S)$ are defined by

$$\mathbf{K}_{\text{Ai}}(x, y) := \int_{\infty e^{-2\pi i/3}}^{\infty e^{2\pi i/3}} d\eta \int_{\infty e^{-\pi i/3}}^{\infty e^{\pi i/3}} d\xi \frac{\exp(\xi^3/3 - \eta^3/3 - x\xi + z\eta)}{\xi - \eta}, \quad (\text{S-106})$$

$$F(\sigma, S) := i^{|S^c|} \oint_{\hat{\Gamma}} \dots \oint_{\hat{\Gamma}} B(\xi; \sigma, S) \prod_{j \in S^c} \left(\frac{\xi_{\sigma(j)} - (2\Delta + i)}{(2i\Delta + 1)\xi_{\sigma(j)} - i} \right)^{\nu(\sigma, S)} \times \prod_{j \in S^c} (i\xi_{\sigma(j)})^{y_j - y_{\tau(j)} - 1} d^{\sigma(S^c)} \xi. \quad (\text{S-107})$$

The definitions of $B(\xi; \sigma, S)$, $\nu(\sigma, S)$, and $\hat{\Gamma}$ are given by Eq. (96), Eq. (97), and Fig. 4 of Ref. [33], respectively.

When s is large, the conjecture approximately leads to

$$\mathcal{F}_N(x, t) \sim \sum_{\sigma \in \mathbb{S}_N} (-1)^\sigma F(\sigma, \phi) + \sum_{\sigma \in \mathbb{S}_N} (-1)^\sigma \sum_{j=1}^N (-1) t^{-1/3} F(\sigma, \{j\}) \mathbf{K}_{\text{Ai}}(s + v_{\sigma(j)}, s + v_j), \quad (\text{S-108})$$

where the first term is unity as proved in Ref. [33]. Thus, the probability $P(|-t - s(t/2)^{1/3}|, t)$ of finding the left-most up-spin for large s can be characterized by the sum of the Airy Kernel. This may be useful for confirming the signature based on our numerical results that this quantity seems to be described by the diagonal Airy Kernel.